ATKINSON-NOLAND & ASSOCIATES
Consulting Engineers • Historic Preservation Specialists

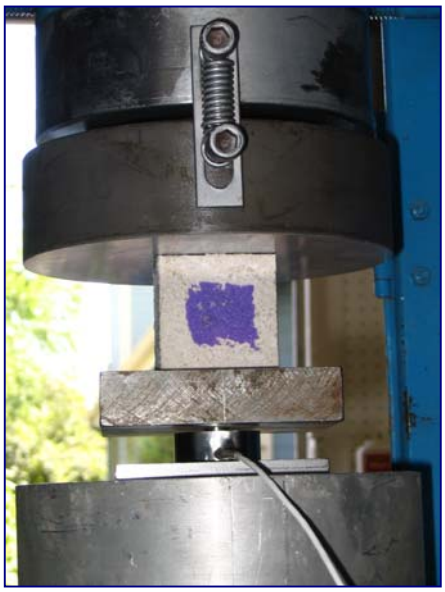

NCPTT GRANT
MT-2210-04-NC-06
FINAL REPORT

Water Transport Characteristics of Masonry Restoration Mortars: Development of a Test Method and a Performance Specification

Atkinson-Noland & Associates

In Collaboration with

Rocky Mountain Masonry Institute
686 Mariposa Street
Denver, CO 80204

December 30, 2005

Atkinson-Noland & Associates, Inc.
2619 Spruce Street
Boulder, Colorado 80302
303 444 3620 • 303 444 3239

TABLE OF CONTENTS

Water Transport Characteristics of Masonry Restoration Mortars: Development of a Test Method and a Performance Specification

1.0 EXECUTIVE SUMMARY

Atkinson-Noland & Associates received funding from the National Center for Preservation Training and Technology grant # MT-2210-04-NC-06 for research to assist in the development of a new ASTM specification for historic mortar. Atkinson-Noland's particular focus in this project was to investigate test methods for determining water vapor transmission (WVT) rates in mortar and to assign appropriate WVT rates for specific hydraulic and non-hydraulic restoration mortars. After review by ASTM, it is intended that the recommendations resulting from this research will be considered for inclusion in the new ASTM specification for mortars for historic masonry. Seven mortar types were tested in this research program in a 1-part binder to 3 part sand ratio:

- Type S Hydrated Lime (HL)
- Lime Putty (LP)
- Type 'O' mortar (1 Portland:2 Hydrated Lime :9 Sand)
- Type 'K' mortar (1 Portland:3 Hydrated Lime:12 Sand)
- Hydrated Hydraulic Lime 2 (HHL_{low})
- Hydrated Hydraulic Lime 3.5 (HHL_{medium})
- Hydrated Hydraulic Lime 5[1] (HHL_{high})

In addition, three substrate materials were tested

- Manitou Sandstone
- Lyons Sandstone
- 'Boulder' pressed brick

We carried out an extensive literature search to survey different methods for determining WVT (see appendix I for annotated bibliography). After a study of several of these methods (see appendix II), we decided upon using the established method as described in ASTM E 96 *Water Vapor Transmission of Material,* using samples cut from mortar

[1] 2, 3.5 and 5 are St. Astier designations indicating minimum compressive strength in MPa

joints, fabricated according to ASTM C 1329. The range of WVT transmission rates of the mortars and substrates are in general agreement with data gathered by others.[2]

One technically challenging aspect of the project was development of a sample curing chamber. Samples must be cured at prescribed temperature and humidity, and have access to ample carbon dioxide, for proper carbonation. The final curing chamber design could be fabricated by testing laboratories using simple, readily available components.

[2] 1) Norman Weiss and Judith Jacob, "Laboratory Measurements of Water Vapor Transmission Rates of Masonry Mortars and Paints", Association for Preservation Technology Bulletin. Vol. XXI No ¾ 1989.
2) Richard Lippoth "Water Vapor Transmission of Various Materials" 2004, Unpublished.

2.0 INTRODUCTION

Direction and degree of water vapor movement in a masonry wall is determined by climatic gradients such as temperature and relative humidity, as well as the nature of the masonry material. It is important to understand the water vapor transmission properties of that mortar in order to ensure compatibility and durability of repair mortar in historic masonry. Water vapor transmission (WVT) will occur predominantly through the more porous material of a given system and the material that carries the greater proportion of water will tend to be the one that deteriorates more quickly. Deterioration resulting from moisture and moisture movement is generally caused by salt crystallization and freeze-thaw cycling. In order to ensure that the mortar and not the masonry units become the sacrificial element in the system, the mortar should have the higher water vapor transmission rate. A bibliography of forty published papers, research reports, and articles related to water vapor transmission and masonry mortar is included in Appendix I. This literature survey includes a brief summary of each of the reviewed publications. .

Atkinson-Noland & Associates has received funding from the National Center for Preservation Training and Technology (NCPTT) to determine appropriate WVT rates for specific hydraulic and non-hydraulic restoration mortars using laboratory methods. This new standard being developed under ASTM committee C12.03.03 will assist in the development of a new ASTM specification for mortar for historic masonry and will describe requirements for repair mortar for historic masonry not addressed in the ASTM C 270 *Standard Specification for Mortar for Unit Masonry.* The ASTM C270 standard exclusively addresses portland cement-based mortars and does not account for differences in the physical properties of lime-based and high-lime mortars.

One of the stated goals of this project was to review the commonly used test method ASTM E 96, *Water Vapor Transmission of Materials* and other standard test methods in order to arrive at an appropriate and highly repeatable method for characterizing the

WVT of mortars (see appendix II). In the course of studying different WVT methods we decided to use the pre-established E96 method in order to insure, or at least increase the likelihood of, repeatability between laboratories.

In addition to WVT testing on mortar samples, we carried out WVT testing on three substrate masonry materials for comparative purposes. These specific substrate materials were chosen because they are frequently used for construction in northern Colorado and represent a range of expected WVT rates. Tested substrate materials include: 1) highly absorptive 'Boulder' pressed brick; 2) low-density Manitou sandstone; and 3) a dense Lyons sandstone.

3.0 MATERIALS

The specific batch information and bulk densities are given below for the materials used in the testing protocol. All materials used conform to their respective ASTM standards.

Portland Cement Type I/II (PC) by QuickCrete serial# 11243964511421.
Bulk density: 94 pcf – (ASTM C 150)

Type S Hydrated Lime (HL) by Chemstar Serial # 3502600011.
Bulk density: 28 pcf - (ASTM C 207)

Lime Putty (LP) by the US Heritage group mixed 3/2004.
Bulk density: 80 pcf - (ASTM C 1489)

Hydrated Hydraulic Lime (HHL) by St. Astier (ASTM C 141)
NHL 2 – Serial # 041980228.
Bulk density: 31 pcf.

NHL 3.5 – Serial # G-04246-11433.
Bulk density: 41 pcf.

NHL 5 – Serial # C-03177-14H38.
Bulk density: 44 pcf.

Mason's Sand by Rio Grande Supply, Denver, CO.
Bulk density: 80 pcf - (ASTM C 144) see Figure 1 below.

The mortar formulations are separated into groups A, B and C, according to the ASTM draft standard as defined by their hydraulicity. Table 1 presents the test matrix:

TABLE 1: MORTAR TYPES AND DESIGNATIONS			
Binder Type	Mortar Mix Designation	Binder Ratio	Sand to Binder Volume Ratio
Type S Hydrated Lime	A1	1 HL	3
Lime Putty	A2	1 LP	3
Hydrated hydraulic lime 2	B1	1 HHL_{low}	3
Hydrated hydraulic lime 3.5	B2	1 HHL_{med}	3
Hydrated hydraulic lime 5	B3	1 HHL_{high}	3
Cement-lime	C1	3 HL :1 PC	3
Cement-lime	C2	2 HL :1 PC	3

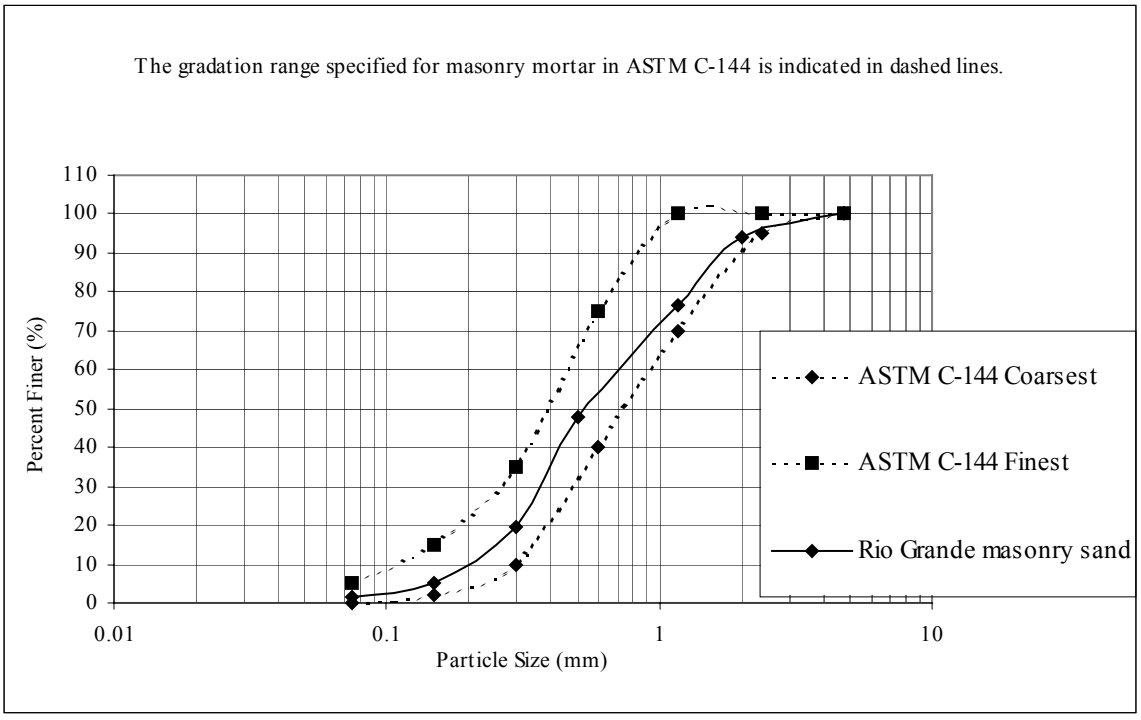

Figure 1 – Particle size distribution of Rio Grande Mason's Sand.

4.0 PREPARATION OF TEST SPECIMENS

4.1 Mixing Procedures

The various binders require slightly different mixing procedures, depending upon their hydraulicity class. The following mixing procedures were followed according to mortar type A, B or C:

Group C Mortars Group C mortar was mixed according to the procedures of ASTM C 305. In short form it reads: place water in bowl, add binder to bowl, mix at low speed and add all sand over 30 seconds, stop, mix at medium speed for 30 seconds. Stop mixer and let mortar sit for 90 seconds, mix at medium speed for 1 minute. Total mixing time is 3½ minutes.

Group A and B Mortars Mixing of Group A and B mortars follow ASTM C 305 with the exception that the initial mixing time is extended to 1 minute to allow for full wetting of the mortar constituents as per the ASTM draft standard C12.03.03. Total mixing time is 4 minutes.

4.2 Plastic Properties

The plastic properties of each mortar batch were tested according to the following ASTM standards to assure batch-to-batch consistency. Results of plastic property tests are presented below in Table 2.

Initial Flow: ASTM C 230 section 10.3, Determination of Flow. For cubes and cylinders, the initial flow was established at 110% ± 5% meeting ASTM C 270. For the mortar joint samples, the flow was established at 125% ± 5% per ASTM C 1329 to allow for anticipated water absorption by the brick (Photo 1). The flow table works by dropping a fixed amount of mortar 25 times in a given amount of time. The slump of the mortar defines the degree of flow.

Water Retention. ASTM C 1506 was used to determine water retention. For our tests, the mercury manometer was replaced with an analog dial vacuum gauge for safety reasons (Photo 2). The apparatus in this test pulls a vacuum on a sample of wet mortar at 7 psi for 1 minute. The sample is then placed on the flow table and its flow recorded. Water retention is expressed as the difference in percentage between the flow of the sample before and after the vacuum has been applied.

Air Content. As per ASTM C 231 the air meter pail technique was used to determine air content. The air pail unit was borrowed from Chemical Lime Corp for a portion of our testing (Photo 3). Note that air content was not measured for all of the test batches.

Vicat Cone Penetration. While this test is recommended in the current C-12.03.03 Protocol, we did not carry it out as we had begun our sample preparation before the protocol recommendations were completed and this test was included. We refer to this test here for reference only (Photo 4)

.

TABLE 2 – COMBINED MORTAR MIXING PARAMETERS AND PLASTIC PROPERTIES

MORTAR TYPE	SAMPLE TYPE	BINDER GRAMS		SAND GRAMS	H_2O ml	FLOW	RETEN-TION	AIR CONTENT
Type S Hydrated Lime	CUBE/CYL	1180		10,000	2500	102	N/A	4.5%
	JOINT	470		4000	1200	110	90%	N/A
Lime Putty	CUBE/CYL	3,333		10,000	850	105	89%	5.5%
	JOINT	1,333		4,000	500	124	N/A	N/A
HHL_1	CUBE/CYL	990		7,650	1,600	112	77%	N/A
	JOINT	660		5,100	1,100	125	73%	N/A
HHL_2	CUBE/CYL	1,650		9,563	2,000	117	61%	6.9%
	JOINT	880		5,100	1,050	122	67%	6.3%
HHL_3	CUBE/CYL	1,725		9,563	1,700	122	40%	7.0%
	JOINT	1,090		6,000	1,000	N/A	N/A	N/A
Type 'K' 3 HL:1 PC	CUBE/CYL	PC 980	HL 1236	10,000	2,400	104	79%	N/A
	JOINT	PC 588	HL 740	6,000	1,600	122	N/A	N/A
Type 'O' 2 HL:1 PC	CUBE/CYL	PC 1388	HL 1166	10,000	2,300	100	N/A	N/A
	JOINT	PC 588	HL 493	4,250	1,500	108	N/A	N/A

PC: PORTLAND CEMENT. HL: HYDRATED LIME TYPE 'S'

Photo 1 – Flow table as per ASTM C 230.

Photo 2 – Vacuum apparatus used for determination of water retention ASTM C 1506.

Photo 3 – Air pail apparatus as per ASTM C 231.

Photo 4 – Vicat penetrometer ASTM C 780.

4.3 Test Sample Preparation.

Three types of test samples were prepared: 1) 2 inch cubes; 2) 2 inch diameter by 4 inch long cylinders and 3) half inch mortar joints. The function of the mortar cubes was solely to carry out compression testing in order to determine 'Standard State' or 75% of full compressive strength. The parameter of standard state was defined in the draft standard as a method for defining the point at which samples should be tested for WVT. Standard state will be further discussed below under compressive strength testing.

Cylinders and joints were fabricated for the various WVT test methods.

2 inch (51 mm) mortar cubes and 2 inch cylinders.

The method for casting mortar cubes and cylinders is described in ASTM C 109. Two inch brass or steel molds were used to fabricate cube samples and 2 inch diameter by 4 inch long plastic cylinders were used to fabricate cylinder samples. Twenty-seven cubes and 12 cylinders of each mortar type were generated (representative sampls shown in Photo 5).

Photo 5 – Mortar samples: cubes, joints and cylinders.

Photo 6 – Mortar joints in fabrication with drop hammer. ASTM C1329.

Mortar Joints

Mortar Joints were fabricated using hard fired clay brick meeting C 216, Grade SW using a mortar joint template described in ASTM C 1329. Bricks were reclaimed from a circa 1910 building to provide suction characteristics representative of historic brick. A doubled piece of cheesecloth was placed between the mortar and the brick to act as a bond-breaker. Mortar was placed in the template and struck with a straight edge. Each joint was compacted using a drop hammer apparatus as described in ASTM C 1329 (Photo 6).

5.0 CURING OF TEST SPECIMENS

Cube, cylinder, and joint samples were tested at intervals throughout the curing cycle to bracket standard state conditions(75% of full compressive strength). The Table below presents anticipated cure ages at testing At the time of this writing, the longest cure time reached for any of the samples has been 120 days.

TABLE 3 - CURING DURATIONS BY MORTAR TYPE.

MORTAR MIX DESIGNATION	BINDER	DAYS CURED AT TESTING								
A1	HL		60	90	120	180	240	300	360	540
A2	LP		60	90	120	180	240	300	360	540
B1	HHL_{low}	28	60	90	120	180	240	300	360	540
B2	HHL_{med}	28	60	90	120	180	240	300	360	540
B3	HHL_{high}	7	14	21	28	42	56	90	120	180
C1	2HL:1PC	7	14	21	28	42	56	90	120	180
C2	3HL:1PC	7	14	21	28	42	56	90	120	180

A constant curing environment is required for proper carbonation of lime components as well as hydration of hydraulic components. Curing of the samples required conditions of 70% ± 5% RH and 72° F according the draft standard. In addition, CO_2 levels had to be maintained close to ambient levels. Relative humidity was controlled in the manner described in ASTM E 104, *Standard Practice for Maintaining Constant Relative Humidity by Means of Aqueous Solutions,* obtained in this case using sodium chloride pellets. Soluble salts regulate relative humidity in closed containers by alternately absorbing and releasing moisture and thereby maintain characteristic vapor pressures. The characteristic RH for sodium chloride is 75.29% at 25 degrees Celsius. Ambient office temperature determined the curing temperature, which occasionally deviated higher or lower than 72° F.

5.1 Curing Chamber

The development of the curing chamber proved to be the most challenging technical aspect of the project. In the course of our research it became apparent that a closed chamber, as required in the ASTM E 104 standard, would not allow the diffusion of carbon dioxide necessary to allow the lime mortar to carbonate. We acquired a CO_2 meter[3] in order to determine the rate of CO_2 consumption by the mortar samples in the chamber. The rate of consumption of the CO_2 was faster than we had anticipated. The data in Figure 2 represents the rate of CO_2 consumption by lime mortar in a closed container full of mortar samples within the first month of their curing cycle. Most of the available CO_2 was consumed in the first hour after closing the chamber.

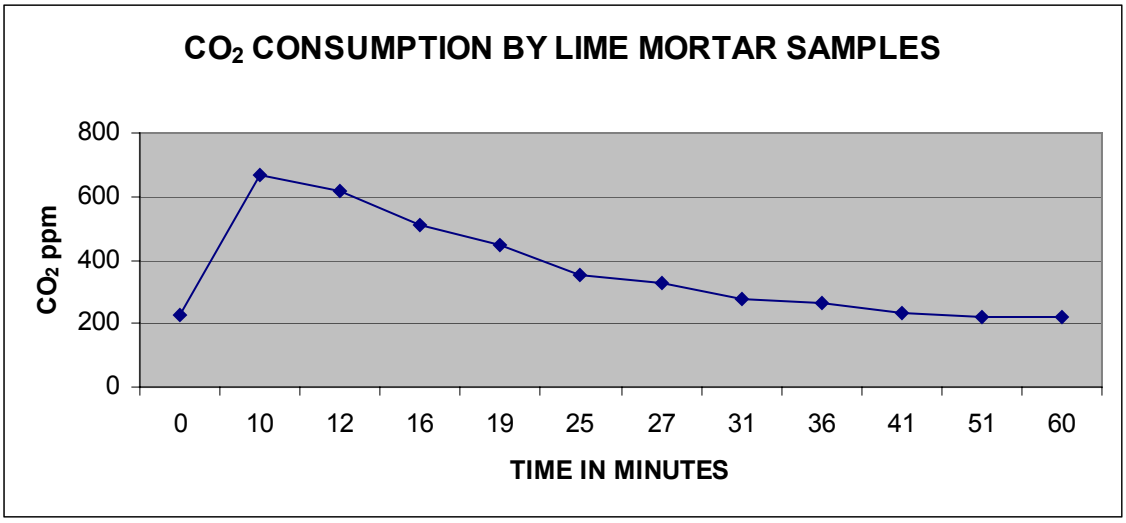

Figure 2 – Consumption of ambient CO_2 in the curing chamber where the peak 700 ppm value occurred after full air exchange by opening the lid. 200 ppm represents the equilibrium value.

Dry ice was added to the curing chamber to increase the level available CO_2. Small dry ice chips were place into an insulated chamber to minimize temperature effects and the insulated box was in turn placed into the curing chamber. CO_2 levels increased dramatically following dry ice addition, exceeding our measurement capability of 10,000 ppm.

[3] Honeywell C7232B Carbon Dioxide Sensor.

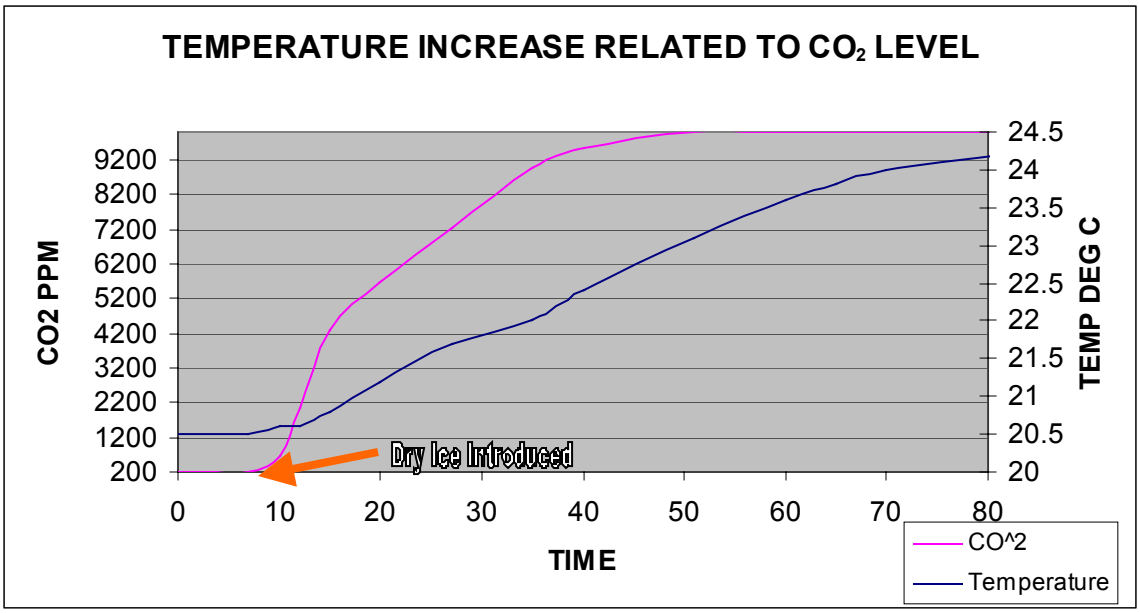

Figure 3 – The chart represents the temperature increase in the curing chamber as a result of the exothermic reaction of the increased CO_2 on the lime samples.

An unanticipated effect of the elevated CO_2 levels was an increase in the temperature within the chamber (Figure 3). Contrary to what we would have expected with the insertion of cold dry ice, the temperature actually increased by 4 degrees centigrade within 80 minutes. We attribute this increase in temperature to an exothermic reaction caused by the carbonation of the lime mortar. While the chemical reaction of carbonation is inherently exothermic, the rate is usually too slow to produce observable temperature increases. In this case, the elevated CO_2 levels generated a discernable temperature increase.

We determined that the exothermic nature of the reaction might change the crystalline structure of the mortar and its physical properties, therefore we did not want to introduce the variable of CO_2 enrichment into the testing protocol. The solution that we settled upon was to cycle ambient air through the chamber for 10 minutes every hour. This resulted in minor fluctuations of CO_2 during curing, but ensured sufficient free CO_2 to complete the curing of the samples.

The problem with this approach was that we quickly lost control of the relative humidity as the NaCl was overwhelmed by the external RH, which tends to be significantly less than 70% in Boulder, Colorado. Our solution to this was to install a humidification apparatus using a humidifier element in a sealed container (Photo 7). In this way, by pre-humidifying the air that was introduced into the chamber, we were able to consistently maintain RH at 70% ± 5%.

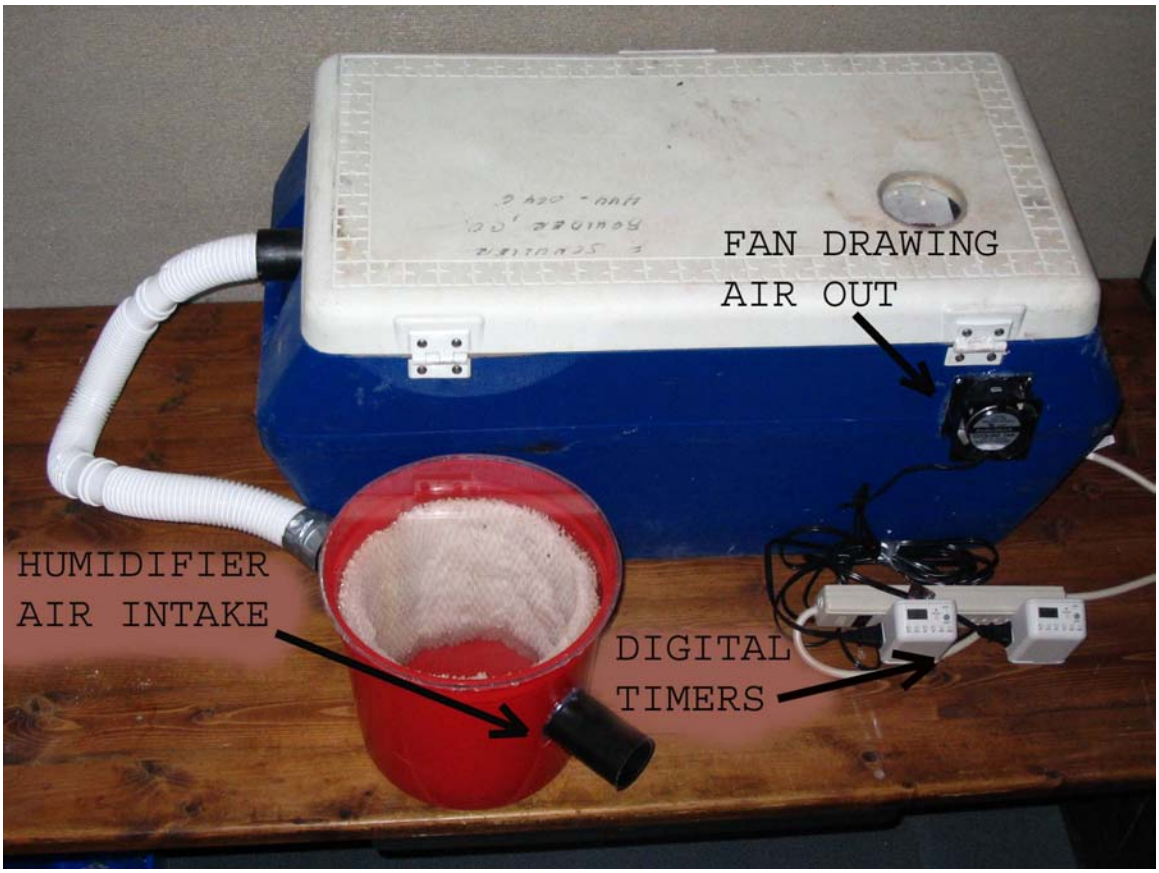

Photo 7 – Curing chamber design.

6.0 TESTING FOR HARDENED PROPERTIES

6.1 Compressive Strength Testing

The interlaboratory testing protocol as established by ASTM subcommittee C12.03.03 defines the standard state of the mortar sample as the point at which it has achieved 75% of its full compressive strength. Mortar cube samples were tested in the Forney compression test machine using a Sensotec load cell[4] (Photos 8 and 9).

Photo 8 – Forney Compression Test Machine.

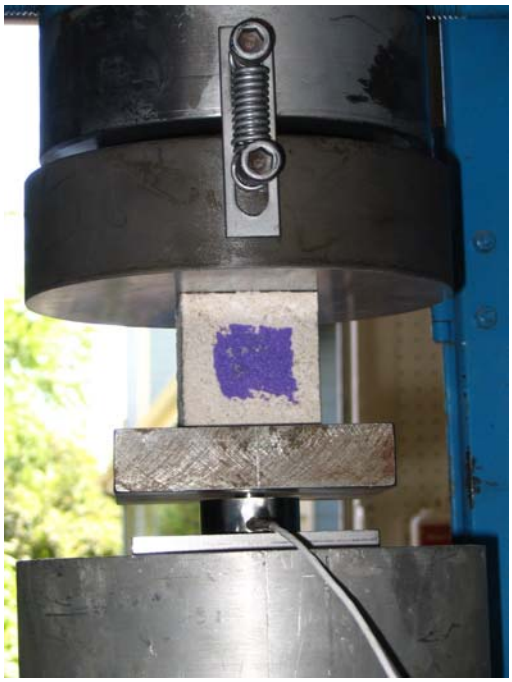

Photo 9 – Detail of sample on the load cell. Sample shows color identifier.

A summary of the compression testing results are presented in Table 4. Plots of all data from compression testing of the 2" cubes are presented in Appendix III.

[4] 0-5000 psi model# 53/239-04-04 serial# 263448.

TABLE 4 - SUMMARY OF COMPRESSIVE STRENGTH RESULTS BY MORTAR TYPE		
MORTAR TYPE	DURATION OF CURE AT TESTING: DAYS	COMPRESSIVE STRENGTH: PSI
Lime Putty	120	125
Hydrated Type S	180	115
Hydrated $Hydraulic_{low}$	180	240
Hydrated $Hydraulic_{med}$	180	280
Hydrated $Hydraulic_{high}$	56	200
Type K (1:3:12)	56	475
Type O (1:2:9)	56	810

6.2 Discussion of Compressive Strength Testing

Compression strength testing is an integral part of this testing protocol as defined by the ASTM draft standard C12.03.03. Compressive strength is easily measured, and can be correlated to other properties such as total porosity or tensile strength. Its importance to mortar for historic masonry is not as important as it is for modern structures, and even then that can be debated. It is presented in the ASTM draft standard as a datum that provides a point for comparison, but not as a goal to be achieved.

Laboratory mortars are cured under specific regimes in order to have a reasonable representation of the mortar once it has reached Standard State (75% of its ultimate strength, total porosity, vapor permeability, and bond potential). Curing conditions are not intended to replicate expected in-service environmental conditions. It is important to understand that lime cures through the reaction of calcium hydroxide or magnesium hydroxide to calcium carbonate or magnesium carbonate. This carbonation does not occur under water-saturated conditions. As the compressive strength of mortars correlates to their degree of curing, strength can be used as an indicator to determine the appropriate time to begin WVT testing. This approach, then, sets an arbitrary but repeatable point where the samples are cured to a significant extent, but taking into account that 100% curing of lime mortar can require years to achieve. We note that a

potential short-coming in this approach is that compression testing is carried out on 2 inch cubes while the mortar that is used for WVT testing is made of the ½ inch samples. The difference in thickness will result in the WVT sample being carbonated to a greater degree than the corresponding cube specimens.

We notice apparent anomalies in several of the samples in that the rate of compressive strength gain decreases during the middle portion of the curing sample. This occurred in four of the seven samples (HHL_{low}, HHL_{med}, 2HL:1PC (type O) and 3HL 1PC (type K)). We theorize that this may have something to do with the relationship between the hardness of the outer, cured core of the sample and the uncured inner core. While not intuitively obvious, a difference in strength between the outer and inner cores may express itself in an overall decrease in strength. This observed behavior has been investigated by the application of Finite Element Method. Results of this study which is included in this report as Appendix IV.

Additional anomalies and loss of data occurred primarily at the beginning of testing due to the compression testing apparatus not having been properly set up and calibrated. Hence some data for curing durations under 60 days are not available.

7.0 WATER VAPOR TRANSMISSION TESTING

A comprehensive literature review was conducted as the first step of the research project. Reviewed publications, listed in Appendix I, revealed there to be many opinions regarding the mechanism of moisture vapor transfer through masonry, and a host of different procedures for conducting vapor transmission tests. Further discussion of the methodologies, equipment, and samples required for the different approaches is included in Appendix II.

In this study, water vapor transmission was measured using the wet cup method described in ASTM E96, *Standard Test Methods for Water Vapor Transmission of*

Photo 10 - WVT test cup preparation showing test cup, cotton ball to prevent splashing of water, ½ inch mortar sample and silicone caulk.

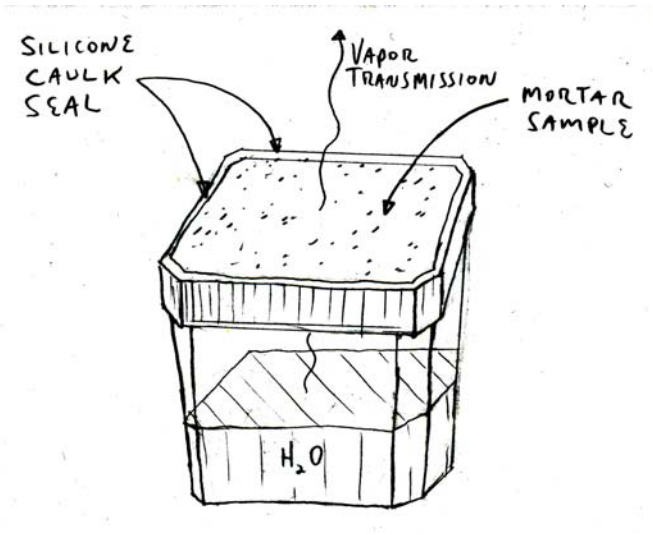

Figure 4 – Design of water vapor test cup with ½ inch mortar sample.

Materials. WVT test specimens were prepared from the mortar joints by cutting 2.25 inch squares with a diamond saw (Photo 10, Figure 4). The containers used were seedling cups purchased at McGuckin's Hardware in Boulder, Colorado. Cotton balls were put into the bottom of the cups to prevent the water from splashing onto the mortar and thus skewing the WVT rates. The mortar samples were sealed to the cups using GE Silicone caulk. Holes were drilled into the sides of the cups, water was injected into the cups and then the holes sealed with silicone caulk.

Magnesium nitrate salt was used to control relative humidity in the closed chamber to approximately 58% (Photo 11). Although the experimental value for relative humidity equilibrium of magnesium nitrate at 25 degrees Celsius is 53%, our RH stabilized at 58%, which is slightly greater than the value of 50% that E96 calls for. Our understanding is that the permeability calculation compensates for variations in RH and

temperature. See 8.2 below for further discussion of water vapor transmission, permeance and permeability.

We are not certain why the salt equilibrated at 58% RH rather than its experimental value of 53%, however, this may have been caused by an insufficient volume of salt or the large number of specimens in the chamber.

Photo 11 – WVT chamber using magnesium nitrate soluble salt to mediate RH.

7.1 WATER VAPOR TRANSMISSION: DISCUSSION OF RESULTS

Results of WVT testing are listed in Tables 5 and 7 and shown in Figure 5. Values from our tests are generally in the range of but slightly less than those recorded by Weiss & Jacob[5] and Richard Lippoth[6] in their research, as listed in Table 6. The difference in the WVT values is most probably due to the fact that our testing was carried out at ambient room temperature of ± 75 degrees Fahrenheit and 58% RH, which varied from the 90 degrees Fahrenheit and 50% RH called for in E 96 and which was followed by the other researchers. While the calculation of Permeance corrects for the difference in temperature and vapor pressure, Lippoth and Weiss/Jacob present their results in WVT.

[5] Norman Weiss and Judith Jacob, "Laboratory Measurements of Water Vapor Transmission Rates of Masonry Mortars and Paints", Association for Preservation Technology Bulletin. Vol. XXI No ¾ 1989.
[6] Richard Lippoth Water, "Vapor Transmission of Various Materials" 2004, Unpublished.

It is difficult to compare our results with those of Lippoth and Weiss/Jacob as they report their results in rate of WVT, which does not take into account variations in sample thickness, temperature, or humidity. In addition, mortar samples were prepared differently by each researcher.

TABLE 5 - COMPARATIVE WATER VAPOR TRANSMISSION, PERMEANCE AND PERMEABILITY VALUES.

MATERIAL TYPE	AVG WVT	PERMEANCE	PERMEABILITY
BRICK	3.5	12.7	7.2
LYONS SANDSTONE	0.8	2.8	1.6
MANITOU SANDSTONE	2.9	10.4	11.3
HHL1	7.2	26.2	12.3
HHL2	5.1	18.4	9.9
HHL3	5.6	20.3	10.5
HLs	7.4	26.8	12.2
LP	7.2	26.1	12.3
2HLs:1PC (O)	5.4	19.7	10.3
3HLs:1PC (K)	5.2	19.0	9.1

TABLE 6 – INTERLABORATORY COMPARISON OF SELECTED WVT DATE

MATERIAL TYPE	ANA AVG WVT	LIPPOTH AVG WVT	WEISS/JACOB
BRICK	3.5		
LYONS SANDSTONE	0.8		
MANITOU SANDSTONE	2.9	6.8	
HHL 1	7.2		
HHL 2	5.1		
HHL 3	5.6		
HL	7.4		
LP	7.2	12	
2HL:1PC ‘O’	5.4	8.5	7.1
3HL:1PC ‘K’	5.2	11	

TABLE 7 – COMBINED ANA WVT TEST DATA										
	BRICK	**LYONS**	**MANITOU**	**HHL1**	**HHL2**	**HHL3**	**HL**	**LP**	**2HL:1PC**	**3HL:1PC**
Avg WVT	**3.5**	**0.8**	**2.9**	**7.2**	**5.1**	**5.6**	**7.4**	**7.2**	**5.4**	**5.2**
Stdev	0.1	0.1	0.2	0.2	0.3	0.2	0.6	0.2	0.4	0.2
Cov(%)	3.0	7.7	8.0	2.7	5.4	3.3	8.1	3.1	7.3	3.1
Avg. Permeance	**12.7**	**2.8**	**10.4**	**26.2**	**18.4**	**20.3**	**26.8**	**26.1**	**19.7**	**19.0**
Stdev	0.4	0.2	0.8	0.7	1.0	0.7	2.2	0.8	1.4	0.6
Cov(%)	3.0	7.7	8.0	2.7	5.4	3.3	8.1	3.1	7.3	3.1
Avg Permeability	**7.2**	**1.6**	**11.3**	**12.3**	**9.9**	**10.5**	**12.2**	**12.3**	**10.3**	**9.1**
Stdev	0.2	0.1	0.9	0.4	0.4	0.5	1.1	0.8	1.0	0.6
COV(%)	2.7	8.4	7.8	3.5	3.9	4.6	8.6	6.6	9.5	6.1

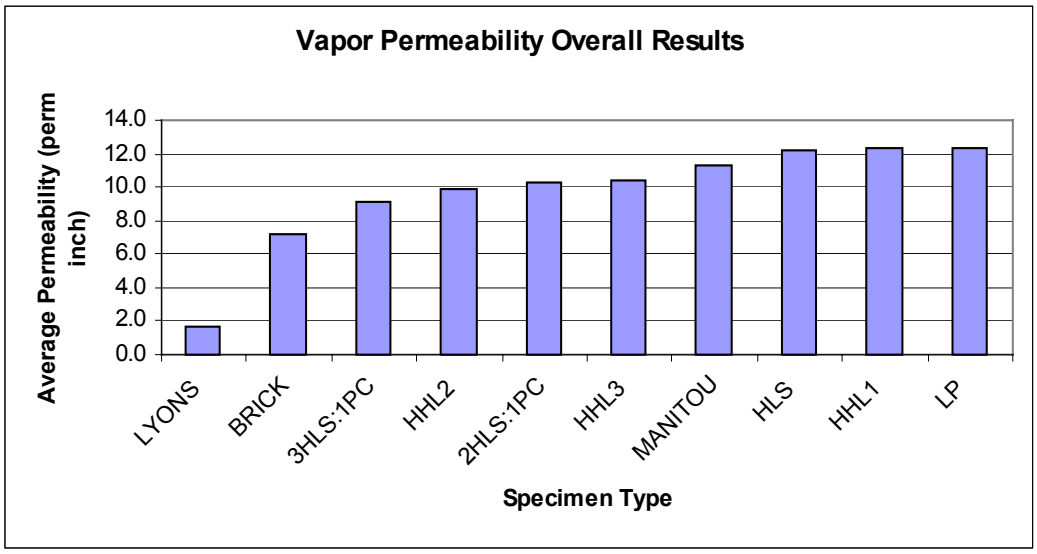

Figure 5 – Comparative vapor permeability values.

The very low standard deviation values presented in Table 7 indicate satisfactory uniformity in the preparation of samples and test cups. Also, the similar values between similar materials, for example HL (hydrated lime) LP (lime putty) and HHL1 (hydrated hydraulic lime – low) reflects a good correlation of experimental results.

7.2 DISCUSSION OF TERMINOLOGY, 'WATER VAPOR TRANSMISSION', 'PERMEANCE' AND 'PERMEABILITY'

The terms 'water vapor transmission', 'permeance' and 'permeability' are often used interchangeably, but they represent different measurements. Water vapor transmission (WVT) expresses the amount of liquid in grams that evaporates through a given surface area over time, expressed in hours ($g/h*m^2$). Permeance is the WVT multiplied by the difference in vapor pressure between the inside and outside of the test cup. Permeability is the permeance multiplied by the thickness of the sample. Permeability is an absolute value and is best used for comparison with data from other testing labs and other materials as it takes into account variables in the environment and in the thickness of the sample. We found that it is often difficult to evaluate results of other research projects such as those of Lippoth and Weiss/Jacob as they report their results in rate of water vapor transmission rather than permeability.

8.0 COROLLARY STUDIES

Appendix IV: Dynamic Young's Modulus Of Elasticity For Masonry Mortars

Dynamic Young's Modulus tests were carried out to investigate the use of nondestructive methods to evaluate the modulus of elasticity of masonry mortar samples. The general testing method was conducted in accordance with ASTM C 215-97, *Standard Test Method for Fundamental Transverse, Longitudinal, and Torsional Resonant Frequencies of Concrete Specimens*. ASTM C 215 explains an approach for measuring Young's Modulus dynamically by exciting a specimen and determining the specimen's resonant frequency. This report is included as Appendix IV. Results were somewhat successful, but there are several recommendations (included in Appendix IV) to improve the success of future applications.

Appendix V: Finite Element Investigation Relating Carbonation Ratio To Compressive Strength For Cast Mortar Cubes

A series of finite element analyses were carried out to determine the effects of various carbonated shell thicknesses on compressive strength of cast mortar cubes. During the

mortar curing process, lime in the mix contributes to compressive strength as it carbonates. Lime carbonation proceeds from the outside cube surface inwards, resulting in creation of a high strength shell surrounding a lower strength (un-carbonated) core. Compression tests indicate that at certain test ages the measured compressive strength levels off or even decreases. The analysis show that the temporary halt in strength gain is related to the carbonated shell phenomenon. Under uniaxial compression loading, the stiffer, carbonated shell resists a disproportionate amount of the applied load, and the associated stress concentrations leads to premature specimen failure. . A complete report is included as Appendix V.

9.0 CONCLUSIONS

The main goal of this testing protocol was to derive accurate and repeatable WVT values for various types of mortars. Obstacles to this goal were greater than anticipated and are outlined here: 1) Small variations in the preparation of test samples affect the WVT characteristics. Such variations include differences in ambient temperature while mixing different batches, air bubbles in the samples, texture variations of the surface of the samples due to the use of cheese cloth as a release material in the casting of joints and variation of joint thickness due to casting irregularities. 2) Variations in curing conditions due to placement of the samples within the curing chamber. The tight fit of the samples in the curing chamber may have potentially created microclimates where the samples were exposed to different relative humidities. 3) Variations in temperature and relative humidity during the WVT testing phase. Our apparatus described in 8.0 was not capable of maintaining perfectly constant temperature or relative humidity. The permeability calculations described in ASTM E96 theoretically compensate for variations in temperature and relative humidity, however actual experimental results may differ due to unanticipated effects. We recommend the use of a more robust WVT testing chamber employing a digitally controlled thermostat and humidification system.

One of the contributions of this project is to have established methods and techniques for future collaborative work to be carried out by other labs. ASTM C12.03.03 is currently organizing work among several labs to build upon the work initiated here. After review by ASTM, it is intended that the recommendations resulting from this research, both described here and carried out by others, will be considered for inclusion in the new ASTM specification for mortars for historic masonry.

One of the main work products of this research project was the development of a procedure for measuring water vapor transmission of masonry mortars. A description of the methodology developed during this project is included in Appendix VII. The methodology was formatted for use by ASTM Committee C12.03.03, to be included in the draft specification currently being developed.

10.0 ACKNOWLEDGEMENTS

This report was developed under a grant from the National Park Service and the National Center for Preservation Technology and Training. Its contents are solely the responsibility of the authors and do not necessarily represent the official position or policies of the National Park Service or the National Center for Preservation Technology and Training.

APPENDIX I
Annotated Bibliography

ANNOTATED BIBLIOGRAPHY

Issues Relating to
Water Vapor Transmission of Mortars

Ait-Mokhtar, Amiri and Sammortino, "Analytic Modeling and Experimental Study of the Porosity and Permeability of A Porous Medium – Application to Cement Mortars and Granitic Rock." *Magazine of Concrete Research.* **51** No. 6 (1999) 391-396.
Summary *Mercury Intrusion Porosimetry and water permeability tests were conducted on mortar and granite samples to determine the relationship between porosity and permeability. No conclusive or apparently practical application resulted.*

Alshamsi, Abdullah, Imran, Hassan, "Development of a Permeability Apparatus for Concrete and Mortar." *Cement and Concrete Research* **32** (2002) 923-929.
Summary *A variant of the standard E 96 test using liquid methanol instead of water. Variabilities of temperature, pressure and mortar mixes were introduced. Test results appeared to show good repeatability potential. As a note however,* Hearn *mentions in "Comparison…" (below) that methanol does react with the products of hydration – and so this solvent might not be ideal.*

Banfill, P.F.G., and A.M. Forester. "A Relationship Between Hydraulicity and Permeability of Hydraulic Lime." *Proceedings of the International RILEM Workshop, Paisley, Scotland*, (12-14 May 1999), (RILEM Publications, France)
Summary *The concept of 'breathability' is defined as the ability to allow moisture which as been absorbed by the fabic to evaporate from the surface. Which is related to the permeability of the material. Numerous tests support the supposition that breathability is inversely proportional to hydraulicity.*

Brown PW, Shi D and Skalny JP "Porosity/Permeability Relationships" *Materials Science of Concrete II* (ed JP Skalny), *American Ceramic Society*, (1992) 83-109.
Not Acquired

Burch, D.M, Thomas, W.C, Fanney, A.H, " Water Vapor Permeability Measurements of Common Building Materials" *ASHRAE Transaction*, (1992), V, 98 pt 2.
Summary *An E 96 test was modified by carrying it out in a desiccant chamber to control RH and temperature. It was determined that the greater the porosity of the material*

being tested, the greater the effect of temperature and RH had on WVT (which is to be expected). This has implications for mortar testing a relatively porous material.

Cabrera, G and C.J. Lynsdale. " A New Gas Permeameter for Measuring the Permeability of Mortar and Concrete." *Magazine of Concrete Research* 40 No 144 (Sept 1988) 177-182.
Summary *The permeability cell described here to test gas permeability of concrete and mortar samples could be applicable to our investigation. The repeatability proved to be very good – some experimental correlation with water vapor permeability will be required. On the whole, a promising technique.*

Cather, R, Figg, J. W., Marsden and T.P O'Brien, "Improvements to the Figg Method for Determining the Air Permeability of Concrete", Magazine *of Concrete Research,* **36**, (129) December 1984, pp 241-245. United Kingdom.
Summary *This in situ method for determining air and water permeability of concrete has been turned into a piece of hardware manufactured by the James Instruments Inc. and called the Poroscope P-6000. The equipment employs an integrated air pressure pump and manometer – battery operated. It would be possible to use the surface kit to test mortar samples in the lab. We plan to use test the equipment in our investigation.*

Charola, Elena and Henriques, FMA "Lime mortars: Some Considerations on Testing Standardization" *Use of and Need for Preservation Standards in Architectural Conservation, ASTM STP 1355 ASTM 1999.*
Summary *A call to standardize preparation of samples and test methods of historic mortars. A discussion of some of the current standards. Recommendations for curing of samples, which include modifications for, lime mortars and increasing the duration of curing up to 4 months. Tests for mortars to be used in historic buildings should not necessarily follow standards tests for modern mortars. They list 'minimum required' and 'desired' tests. Minimum required include: 1) Water vapor permeability 2) capillary water absorption 3) soluble salt content and 4) drying shrinkage.*

Charola A. E. and F. M. A. Henriques "Hydraulicity in Lime Mortars Revisited." *Proceedings of the International RILEM Workshop, Paisley, Scotland*, (12-14 May 1999), (RILEM Publications, France)
Not Acquired

Chou Chen, L. and D. L. Katz. "Diffusion of Methane Through Concrete". ACIJ. **75** No. 12 (1978) 673-679.

Summary *The diffusion of methane gas through wet and dry concrete was measured. Not necessarily useful for this investigation.*

Depraetere, W. J. Carmeliet and H. Hens. "Moisture Transfer at Interfaces of Porous Materials: Measurements and Simulations". *Proceedings of the International RILEM Workshop, Paisley, Scotland*, (12-14 May 1999), (RILEM Publications, France)
Summary *Four contact phenomena are described at the interface between mortar and brick which can significantly change moisture behavior of historic masonry: 1) perfect hydraulic contact2) an airspace between two materials 3) a natural contact and 4) a real contact. The subtle differences between these phenomena are lost on me and the subject of the paper might be useful in general – but not for this particular project.*

Dinku, Abeb, H.W. Reinhardt. "Gas Permeability Coefficient of Cover Concrete as a Performance Control." *RILEM* **30** (Aug-Sept 1997) 387-391.
Summary *The authors employ the 'over pressure' method to determine the gas permeability of concrete either in situ or in the lab. The apparatus appears similar to the Poroscope P-6000. Maybe a useful method for concrete slab but not practical for mortar samples of lesser depth.*

El-Dieb, A.S., Hooton, R.D., "Evaluation of the Katz-Thomson Model for Estimating the Water Permeability of Cement-Based Materials from Mercury Intrusion Porosimetry Data," Cement *and Concrete Research,* **24** No. 3 (1994) 443-455.
Summary *A review of the theory of Mercury Intrusion Porosimetry and it's refinement by the Katz-Thompson theory. As porosity is only one of many parameters affecting permeability, MPI will probably not be a useful general test for WVT determination. MIP has limited use for our investigation.*

Figg, JW "Methods of Measuring the Air and Water Permeability of Concrete." *Magazine of Concrete Research,* **25** No. 85 December (1973) 213-219.
Not Acquired

Figg, John, "Concrete Surface Permeability: Measurement and Meaning." *Chemistry and Industry (London)* 6 November 1989, pp 714-719 United Kingdom.

Not Acquired

Goins E. "A new protocol for the analysis of historic cementitious materials: interim report." *Proceedings of the International RILEM Workshop, Paisley, Scotland*, (12-14 May 1999), (RILEM Publications, France)
Not Acquired

Goueygou, M., Lafhaj, Zoubeir. "Relationship Between Porosity, Permeability and Ultrasonic Parameters in Sound and Damaged Mortar" *International Symposium: Non-destructive Testing in Civil Engineering*, 2003.
Summary *The study intended to relate physical parameters (porosity and permeability) and acoustical parameters (pulse and phase velocity, attenuation) of sound and damaged, dry or water saturated mortar samples. In general, phase and pulse velocity decrease with porosity due to air voids (as would be expected). The study highlights the difficulty of obtaining accurate estimates of ultrasonic parameters because of the large number of variables. This will probably not be a useful direction for our investigation.*

Groot C.J.W.P., P. Bartos, J.J. Hughes "Characterization of Old Mortars with Respect to their Repair." *Proceedings of the 12th International Brick/Block Masonry Conference, Madrid*. (June 2000) 815-827.
Not Acquired

Groot C. J. W. P., P. J. M. Bartos and J. J. Hughes "Historic Mortars: Characteristics and Tests - Concluding summary and state-of-the-art." *Proceedings of the International RILEM Workshop, Paisley, Scotland*, (12-14 May 1999), (RILEM Publications, France)
Not Acquired

Hearn N., R.J. Detwiler, C. Sframeli "Water Permeability and Microstructure of Three Old Concretes, *Cement and Concrete Research.* **27** No. 5 (1997) 761-755.
Not Acquired

Hearn, N. *"Comparison of Water and Propan-2-ol Permeability in Mortar Specimens."* Advances in Cement Research **8** No. 30 *(1996).*
Summary *The purpose of the study was to compare water permeability with a non-reactive permeant propan-2-ol (aka isopropyl alcohol). Propan-2-ol was chosen as a permeant in order to avoid continuing hydration and dissolution of hydrates. A complex*

'solvent replacement' technique is described, to displace water by the alcohol. A modified version could be useful for our investigation.

Henriques, FMA, "Testing Methods for the Evaluation of New Mortars for Old Buildings," *Science and Technology for Cultural Heritage,* Vol. 5, No 1 (1996). 57-61.
Not Acquired

Henriques, FMA and Charola AE, Comparative Study of Standard Test Procedures for Mortars," *Proceedings of the 8th International Congress on Deterioration and Conservation of Stone.* J Riederer, Ed., Moeller Druck und Verlag, Berlin, (1996) 1521-1528.
Summary *The various standard procedures for testing mortars result in very different properties. Samples were prepared according to RILEM and NORMAL specs and properties such as compressive, flexural strength, modulus of elasticity and water absorption varied widely. The conclusion is a call for international standardization*

Hughes, D.C., "Pore Structure and Permeability of Hardened Cement Paste." *Magazine of Concrete Research.* **37** No.133 (1985) 227-233.
Not Acquired

Loosveldt, Helene, Zoubeir Lafhaj, Frederic Skoczylas. "Experimental Study of Gas and Liquid Permeability of a Mortar." *Cement and Concrete Research* ***32*** (2002) 1357-1363.
Summary *This is potentially a very useful article comparing the liquid and gas permeability of mortar. In samples cored from the same mortar, water permeability (using a pressure cell) was half that of gas (argon), ethanol was somewhere between. Nevertheless, ethanol and gas were found to have similar permeability when Klinkenberg or slippage effect was taken into account. The results of water permeability testing can be affected by 1) rehydration of non-reacted cement, 2) dissolution/preciptiation, migration of fine elements and water adsorption in the smallest pores of the cement matrix.*

Mosquera, M.J., Benitez, D, Perry, S.H., "Pore Structure in Mortars Applied on Restoration Effect on Properties Relevant to Decay of Granite Buildings," *Cement and Concrete Research* **32** (2002) 1883-1888.
Summary *The focus of the paper is to characterize the pore structures of a set of mortars and correlate them with mechanical properties and vapor permeability. A good correlation was found between total porosity and the two parameters tested, strength and vapor diffusivity. Vapor transport was measured using a sensitive balance, which measured the mass change of a mortar sample inside of an environmental chamber. Mortars with lime had significantly greater vapor permeability than those without.*

Ollivier, J. P. and M. Massat. "Permeability and Microstructure of Concrete: A Review of Modeling." *Cement and Concrete Research* **22** (1992) 503-514.
Summary This statistical approach attempts to predict water and water vapor permeability of concretes and mortars by determining their pore size distribution and tortuosity by MIP. Many experimental difficulties were encountered – probably not a useful direction for our investigation.

Reinhardt, W, K. Graber "From Pore Size Distribution to an Equivalent Pore Size of Cement Mortar." *Materials and Structures,* **23** (1990) 3-15.

Summary Similar to the Ollivier article, a relationship between pore size distribution and permeability is demonstrated. These authors claim success, but the MIP method used here is probably not suitable for our purposes.

Schonlin, K., H. K. Hilsdorf. "Permeability as a Measure of Potential Durability of Concrete – Development of a Suitable Test Apparatus." *Permeability of Concrete, AIC* (1988)
Summary The authors present a new cell for determination of gas permeability. The diagram is not as clear as it could be on fabrication details. Testing of concrete of varying cure times and mix ratios seemed to give good correlation with permeability values.

Schuller, Michael P. Robert S.K. van der Hoeven, Margaret Thomson. "Comparative Investigation of Plastic Properties and Water Permeance of Cement-Lime Mortars and Cement-Lime Replacement Mortars." *Water Problems in Building Exterior Walls ASTM STP 1352 (1998).*
Summary Useful references for ASTM tests required for our current investigation.

Sickels-Taves, Lauren, B, Michael S. Sheehan. "Specifying Historic Materials: The Use of Lime." *Masonry: Opportunities for the 21st Century*." ASTM STP 1432 (2002) 3-23.
Summary Good overview of the use of lime in restoration mortars and the problems associated with the use of Portland cement. Discussion of the need for greater industry and public awareness for its use. Useful information on the current research and specification procedure.

Thomson, Margaret L and Godbey Richard, J. "Effect of Adding Hydrated Lime to Masonry Cement Mortar on Physical Properties" North *American Masonry Conference, Clemson, South Carolina.* (June 1-4, 2003) 1012-1021.
<u>Summary</u> *The authors promote the introduction of ASTM standards to allow addition of hydrated lime to modify mortar properties. Rationale for inclusion of lime includes the beneficial decrease of compressive strength, decrease of modulus of elasticity (becomes more elastic) increases bond strength, increases water retention, decreases water penetration.*

Thomson, M.L., L. Fontaine, G.T. Suter. "Practice and Research: The Need for Standards for Historic Mortars." *The Use of and Need for Preservation Standards in Architectural Conservation, ASTM STP 1355* (1999).
<u>Summary</u> This *paper discusses the limitations of current standards regarding the testing and application of historic mortars and particularly the durability of such mortars. Lack of standardized vapor permeability testing is cited as one of the significant obstacles to standardizing historic mortars. Other issues include the need for modification of the Vicat test for drier mortars, modification of the flow test, modification of air content tests for drier mixes and shorter testing times from 28 to 7/14 days. Five performance criteria were defined including: 1) Compressive strength 2) Split tensile strength 3) Modulus of elasticity 4) Flexural bond strength 5) Expansion (freeze-thaw test) of masonry.*

Thomson, M.L., and Caspar Groot. "Rilem TC Characterization of Old Mortars with Respect to their Repair." *The Use of and Need for Preservation Standards in Architectural Conservation, ASTM STP 1355* (1999).
<u>Summary</u> *This is an interim report on the work accomplished by the RILEM technical committee, established in the fall of 1996 to 1) characterize old mortars for the purpose of reproduction 2) identification of parameters and standardization for testing methods. Work has been completed in definition and classification of mortars, chemical and physical characterization of mortars, standard methods of characterizing mortars with respect to their performance in situ. Quality control procedures for mortars.*

Thomson, M.L. and Richard Godbey. "Proportioning Cement – Lime Masonry Mortar Mix Designs Using Water Retention Testing for the Purpose of Improving Mortar Workability." *North American Masonry Conference.* (2003) 1043-1051.
<u>Summary</u> *A comprehensive discussion of the parameters and requirements for workability of historic mortars. Water retention of mortars is examined as means to improving the workability of mortars involving problematic sand (non-conformance to C-144). Variables contributing to workability include water content, aggregate type and size and admixtures. Problems with non-conformance to C 144 –gradation of sand*

particle size and its effect on the characteristics of mortar are discussed. Addition of lime to the mix – as little as 2% by batch weight can improve workability.

Thomson M. L. "Plasticity, Water Retention, Soundness and Sand Carrying Capacity: What a Mortar Needs." *Proceedings of the International RILEM Workshop, Paisley, Scotland*, (12-14 May 1999), (RILEM Publications, France)
Summary *A description of the necessary properties of mortar (listed in the title) and the demonstration that the addition of lime to the mortar generally increases all of these properties.*

Valek J., Hughes J.J. and Bartos P.J.M**.** "Gas Permeability, Moisture Content and Carbonation of Conservation Lime Mortar." *Proceedings of the Euromat Conference, Vol. 6 Materials for Buildings and Structures*, Munich, (Sept-Oct 1999), 209-215,
Summary *The paper connects problems with the use of lime mortars in conservation and the most recent research in vapor transport phenomena. Two hypotheses are suggested: 1) the gas permeability of lime mortars is influenced more by surface finish than the amount of water added to the mix. 2) The carbonation process of lime mortars depends on the surface gas permeability rather than the internal gas permeability. Surface permeability may be the rat- determining factor. Important reference to a permeability device presented at the Paisley conference.*

Valek, Jan, John Hughes, Peter Bartos. "Portable Probe Gas Permeametry in the Testing of Historic Masonry and Mortars." *Proceedings of the International RILEM Workshop, Paisley, Scotland*, (12-14 May 1999), (RILEM Publications, France).
Summary *A portable probe gas permeameter was used for the analysis of mortar and stone. The paper discusses advantages and disadvantages of the method, outlines the practicalities of the test equipment and proposes how the method can be used in practical conservation of historic masonry. Inquires to various manufacturers placed the cost at around $25K.*

Van Brakel, J "A Special Issue Devoted to Mercury Porosimetry. *Powder Technology* 29 No. 1 (1981) 1-209
Not Acquired

van Balen. K., E.-E. Toumbakari,M.-T. Blanco-Varela, J. Aguilera, F. Puertas, C. Sabbioni, G. Zappia, C. Riontino and G. Gobbi "Procedure for a Mortar Type Identification: a Proposal" *Proceedings of the International RILEM Workshop, Paisley, Scotland*, (12-14 May 1999), (RILEM Publications, France)

Summary A discussion of various techniques for the identification of historic mortars including optical microscopy, x-ray diffraction, chemical composition. Not particularly useful for our investigation.

APPENDIX II
TEST PLAN
FEBRUARY 2005

Atkinson-Noland &Associates
Mortar Water Vapor Transmission Research
Summary of proposed work
By Peter Champe of ANA

In support of the development of
STANDARD SPECIFICATION
FOR MORTARS FOR HISTORIC
MASONRY,
ASTM Committee C12.03.03

I. Introduction

Direction and degree of water vapor movement in a masonry wall is determined by climatic gradients such as temperature and relative humidity, as well as the nature of the masonry material. Water vapor transmission in masonry occurs dominantly through the mortar joint rather than the masonry unit. It is important, therefore, in order to ensure compatibility and durability of a mortar repair to historic masonry to understand the water vapor transmission properties of that repair mortar. Atkinson-Noland & Associates has received funding from NCPTT to research and investigate by laboratory testing the most appropriate standard method for measuring water vapor transmission (WVT) on a broad range of mortar types that might be used as repair mortar to historic masonry. In addition, by completing a comparative interlaboratory study the work is expected to provide a basis to assign appropriate WVT rates for specific repair mortars composed of specific binder components. This research will assist in the development of a new ASTM specification for mortar for historic masonry. This new standard will describe requirements for repair mortar for historic masonry not addressed in the ASTM C 270 *Standard Specification for Mortar for Unit Masonry*.

In our investigation, we will review the commonly used test method ASTM, E 96 Water Vapor Transmission of Materials and other standard test methods in order to arrive at an appropriate and highly repeatable method for characterizing the WVT of mortars. We are revisiting the appropriateness of

the E 96 method for a number of reasons. One of the most common complaints lodged against the E 96 method is the lack of repeatability (in the same laboratory) and reproducibility (between laboratories). The reasons for this may include variations in environmental conditions during curing or testing of the samples. There may also be some inconsistency inherent to the E 96 test such as:

1) rehydration of non-reacted hydraulic components,
2) dissolution/precipitation of soluble phases and migration of fine elements in the mortar matrix, and
3) water adsorption in the smallest pores of the mortar matrix

These variations may be traced to the water-based testing employed by E 96. An additional drawback of E 96 is its duration, which can require several weeks of testing before final results are available. This can be a significant obstacle for projects on real-life construction schedules.

II. Materials

The following mortar types will be prepared as part of the research program.

Mortar Batch Number	Binder Type	Binder/Sand Ratio
1	C 270 Type O cement-lime	1:3
2	C 270 Type K cement-lime	1:3
3	calcined hydraulic lime 300 psi	1:3
4	calcined hydraulic lime 500 psi	1:3
5	calcined hydraulic lime 725 psi	1:3
6	Lime Putty	1:3
7	Hydrated Lime	1:3
8	blended hydraulic lime	1:3

In addition to the mortar, we will test samples of:

1) brick (extruded, hand molded and hydraulic pressed)
2) stone (Manitou sandstone, granite and limestone) for comparative purposes.

Material types and sources are listed on the attached data sheets. A natural sand will be locally obtained. The sand is largely silica based, is within the requirements of ASTM C 144, and has the gradation shown below.

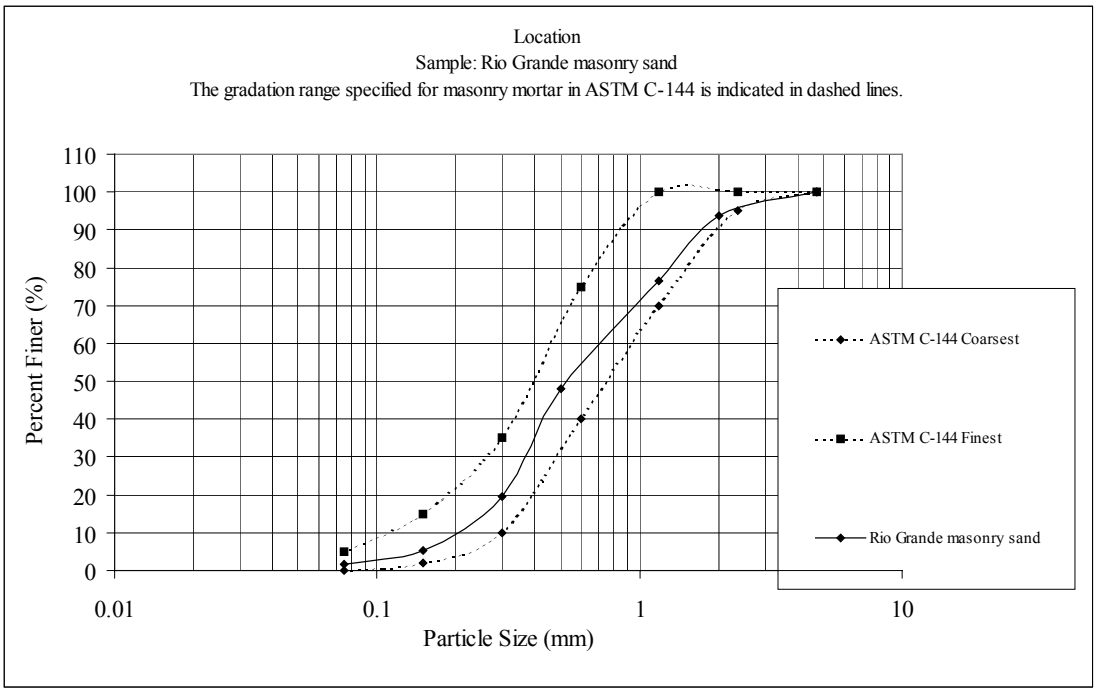

III. Test Methods.

Plastic Properties: The following tests to characterize plastic properties will be carried out for each mortar sample:

- Air content as per ASTM C 780
- Water retention as per ASTM C 1506
- Flow as per ASTM C 230

Curing Conditions: Following the recommendations of the draft standard, hydraulic-based mortars will be cured in 100% Relative Humidity (RH) and lime-based mortars will be cured in a 70% ± 5% RH. Water vapor transmission testing will be carried out on mortars cured to Standard State,

defined as a test sample having cured to achieve at least 75% of its final, fully cured compressive strength.

Hardened Properties: The following tests to characterize hardened properties will be carried out for each mortar type:

- Compression Strength as per ASTM C 109. (This test will define the Standard State for each mortar type.)
- Modulus of Elasticity as per ASTM E1875-00e1 Standard Test Method for Dynamic Young's Modulus, Shear Modulus, and Poisson's Ratio by Sonic Resonance.
- Water vapor transmission (see discussion below).
- Mercury Intrusion Porosimetry. (Selected mortar samples will be sent to another laboratory for MIP testing.).

IV. Water Vapor Transmission Testing

Specimens for WVT testing will be prepared in two ways: 1) by cutting discs from 2″ x 4″ cylinders and 2) by taking mortar joints prepared by using the method described in Section 7.9 of the proposed ASTM draft specification. (this using a cheese cloth as a joint break between the masonry units). Our initial test series will investigate the viability of these two approaches of sample preparation.

Modified E 96 with Alcohol – In addition to the standard E96 WVT testing using water, we will carry out modified versions using alcohol. Three studies

investigating water vapor transmission in mortar and concrete samples 1) Alshamsi and Imran (2002)[1] 2) Hearn (1996)[2] and 3) Loosveldt et al., (2002)[3]demonstrated acceptable repeatability using alcohol instead of water in modified E 96 tests. The potential advantages of using water free-alcohol instead of water include less reactivity with the hydraulic mortar components as well as alcohol's greater vapor pressure, which could accelerate the testing procedure. Alshamsi and Imran (2002) uses methanol as the permeant, however, Hearn (1996) notes that methanol has some reactivity with calcium hydroxide and suggests the use of propan–2-ol (isopropyl alcohol).

Poroscope P-6000 A proprietary instrument, the Poroscope P-6000 (James Instruments) may be useful in the determination of water or air permeability, which can then be correlated to WVT. The equipment is specifically designed for testing concrete slabs *in situ* and can be used in two ways: either by drilling a hole in the slab, plugging the hole and introducing water or air under pressure (which may not be applicable to mortar) or applying a surface seal (which is probably more applicable to our purposes).

The Poroscope also has some promise for conducting *in situ* measurements of masonry unit (and possibly mortar) permeability. The objective of this research component is to correlate Poroscope measurements with WVT measured using laboratory procedures for future use as a field evaluation methodology.

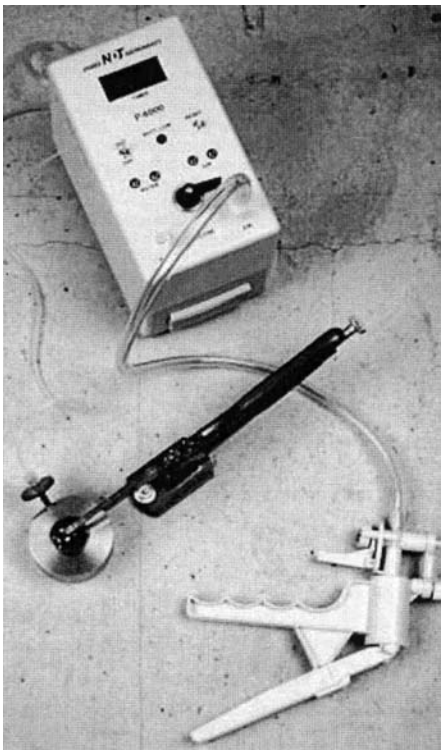

Figure 1

The Poroscope unit shown here (Figure 1) is outfitted with the surface testing kit, which would be required for testing mortar joint specimens.

Constant or Falling Head Permeameter – This method based on ASTM D5856 Standard Test Method for Measurement of Hydraulic Conductivity of Porous Material

Using a Rigid-Wall, Compaction-Mold Permeameter is most commonly used in soil permeability analysis, but may be adaptable to test the permeability of mortar cores. The amount of water passing through a sample over a given

time will provide a water permeability rate. It will be necessary to correlate the liquid movement of water through the sample with WVT as these are

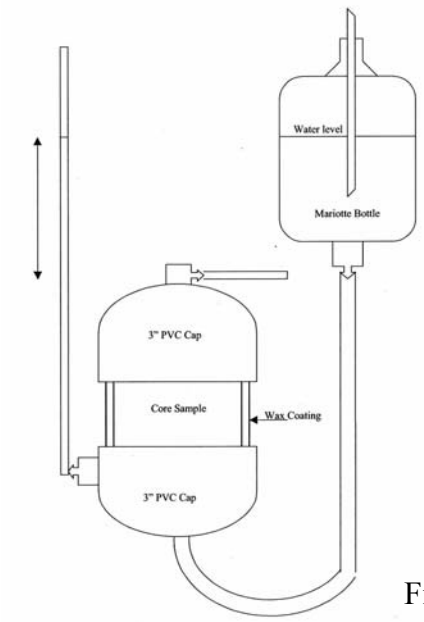

Figure 2

slightly different mechanisms. This method would be used for rapid evaluation of mortar permeability using equipment common to many commercial testing laboratories. (Figure 2)

Gas Permeameter Test Cell Method – the 'Leeds Cell'

G. Cabrera and C. J. Lynsdale present a new test cell method in their article "A New Gas Permeameter for Measuring the Permeability of Mortar and Concrete"(need to clean up reference) illustrated above. Leeds refers to the University of Leeds where the cell was developed. The advantages of this

method are the following: 1) after drying the samples for 24-36 hours, the permeameter testing only requires about 30 minutes; 2) a high degree of repeatability (so indicated in their article) not closely dependent on variables such as ambient temperature and humidity; 3) small samples can be taken from actual structures. Considerations include: 1) the complexity of the apparatus and preparation of the samples, which may or may not render it appropriate as an ASTM specification; 2) the correlation of the gas permeability with water vapor permeability, which will have to be

Figure 3

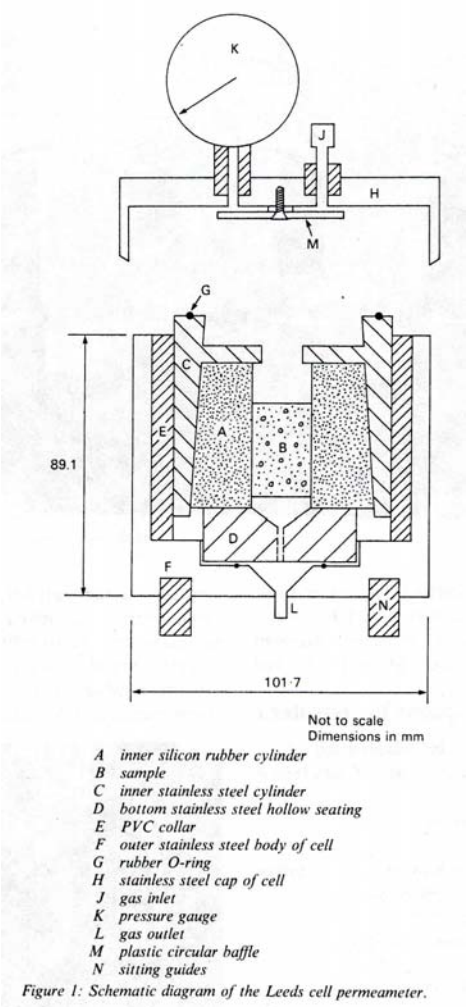

Figure 1: Schematic diagram of the Leeds cell permeameter.

Figure 4

determined experimentally. (Figures 3 & 4)

V. Test Plan

The following charts summarize the proposed mortar materials and associated tests to be carried out.

1 Quickcrete Portland I/II serial # 11243964511421
2 Chemstar Type S Lime serial # 3502600011
3 "Mason's Sand" supplied by Rio Grande Conforming to ASTM C 144
4 St Astier NHL 2: Serial # 041980228
5 St Astier NHL 3.5: Serial # G - 04246-11433
6 St Astier NHL 5: Serial # C-03177-14H38
7 Lime Putty supplied by U.S. Heritage Group, Inc. Mixed 3/2004.
8 Metakaolin (PowerPozzTM) produced by Advanced Cement Technologies, LLC

Type 'S' Lime - 1:3 **Testing at Standard State** (assumed 180 Days)

Age	Compressive Strength	Elastic Mod.	**WVT**				
	C 109 (determines	Dynamic Modulus	ASTM E 96	E 96 Modified	Leeds -	Poroscope	Falling Head Permeameter
	Standard State)	ASTM E1875		W/ Isopropyl	Air Perm Cell	(Proprietary)	ASTM D5856-95(2002)e1
	Quant/	*Quant/*	*Quant/*	*Quant/*	*Quant/*	*Quant/*	*Quant/*
	Type	*Type*	*Type*	*Type*	*Type*	*Type*	*Type*
28	3/cube						
56	3/cube						
84	3/cube						
112	3/cube						
175	3/cube	3/cyl	2/cyl and	2/cyl and	2/cyl	2/cyl	2/cyl
364	3/cube		joint	joint			

Atkinson-Noland &Associates
Mortar Water Vapor Transmission Research
Summary of proposed work
By Peter Champe of ANA

In support of the development of
STANDARD SPECIFICATION
FOR MORTARS FOR HISTORIC
MASONRY,
ASTM Committee C12.03.03

Type 'O' Hydraulic - 1:3 **Testing at Standard State** (assumed 28 days)

Age	Compressive Strength	Elastic Mod.	**WVT**				
	C 109 (determines	Dynamic Modulus	ASTM E 96	E 96 Modified	Leeds -	Poroscope	Falling Head Permeameter
	Standard State)	ASTM E1875		W/ Isopropyl	Air Perm Cell		ASTM D5856-95(2002)e1
	Quant/	*Quant/*	*Quant/*	*Quant/*	*Quant/*	*Quant/*	*Quant/*
	Type	*Type*	*Type*	*Type*	*Type*	*Type*	*Type*
7	3/cube						
14	3/cube						
28	3/cube	3/cyl	2/cyl and	2/cyl and	2/cyl	2/cyl	2/cyl
56	3/cube		joint	joint			
84	3/cube						

Type 'K' Hydraulic - 1:3 **Testing at Standard State** (assumed 28 days)

Age	Compressive Strength	Elastic Mod.	**WVT**				
	C 109 (determines	Dynamic Modulus	ASTM E 96	E 96 Modified	Leeds -	Poroscope	Falling Head Permeameter
	Standard State)	ASTM E1875		W/ Isopropyl	Air Perm Cell		ASTM D5856-95(2002)e1
	Quant/	*Quant/*	*Quant/*	*Quant/*	*Quant/*	*Quant/*	*Quant/*
	Type	*Type*	*Type*	*Type*	*Type*	*Type*	*Type*
7	3/cube						
14	3/cube						
28	3/cube	3/cyl	2/cyl and	2/cyl and	2/cyl	2/cyl	2/cyl
56	3/cube		joint	joint			
84	3/cube						

CHL 300 - 1:3 **Testing at Standard State** (assumed 84 Days)

Age	Compressive Strength	Elastic Mod.	**WVT**				
	C 109 (determines	Dynamic Modulus	ASTM E 96	E 96 Modified	Leeds -	Poroscope	Falling Head Permeameter
	Standard State)	ASTM E1875		W/ Isopropyl	Air Perm Cell	(Proprietary)	ASTM D5856-95(2002)e1
	Quant/	*Quant/*	*Quant/*	*Quant/*	*Quant/*	*Quant/*	*Quant/*
	Type	*Type*	*Type*	*Type*	*Type*	*Type*	*Type*
28	3/cube						
56	3/cube						
84	3/cube	3/cyl	2/cyl and	2/cyl and	2/cyl	2/cyl	2/cyl
112	3/cube		joint	joint			
175	3/cube						
364	3/cube						

Atkinson-Noland &Associates
Mortar Water Vapor Transmission Research
Summary of proposed work
By Peter Champe of ANA

In support of the development of
STANDARD SPECIFICATION
FOR MORTARS FOR HISTORIC
MASONRY,
ASTM Committee C12.03.03

CHL 500 - 1:3 **Testing at Standard State** (assumed 56 days)

Age	Compressive Strength	Elastic Mod.	**WVT**				
	C 109 (determines	Dynamic Modulus	ASTM E 96	E 96 Modified	Leeds -	Poroscope	Falling Head Permeameter
	Standard State)	ASTM E1875		W/ Isopropyl	Air Perm Cell		ASTM D5856-95(2002)e1
	Quant/	*Quant/*	*Quant/*	*Quant/*	*Quant/*	*Quant/*	*Quant/*
	Type	*Type*	*Type*	*Type*	*Type*	*Type*	*Type*
7	3/cube						
14	3/cube						
28	3/cube						
56	3/cube	3/cyl	2/cyl and	2/cyl and	2/cyl	2/cyl	2/cyl
84	3/cube		joint	joint			

CHL 750- 1:3 **Testing at Standard State** (assumed 56 days)

Age	Compressive Strength	Elastic Mod.	**WVT**				
	C 109 (determines	Dynamic Modulus	ASTM E 96	E 96 Modified	Leeds -	Poroscope	Falling Head Permeameter
	Standard State)	ASTM E1875		W/ Isopropyl	Air Perm Cell		ASTM D5856-95(2002)e1
	Quant/	*Quant/*	*Quant/*	*Quant/*	*Quant/*	*Quant/*	*Quant/*
	Type	*Type*	*Type*	*Type*	*Type*	*Type*	*Type*
7	3/cube						
14	3/cube						
28	3/cube						
56	3/cube	3/cyl	2/cyl and	2/cyl and	2/cyl	2/cyl	2/cyl
84	3/cube		joint	joint			

Lime Putty - 1:3 **Testing at Standard State** (assumed 180 Days)

Age	Compressive Strength	Elastic Mod.	**WVT**				
	C 109 (determines	Dynamic Modulus	ASTM E 96	E 96 Modified	Leeds -	Poroscope	Falling Head Permeameter
	Standard State)	ASTM E1875		W/ Isopropyl	Air Perm Cell	(Proprietary)	ASTM D5856-95(2002)e1
	Quant/	*Quant/*	*Quant/*	*Quant/*	*Quant/*	*Quant/*	*Quant/*
	Type	*Type*	*Type*	*Type*	*Type*	*Type*	*Type*
28	3/cube						
56	3/cube						
84	3/cube						
112	3/cube						
175	3/cube	3/cyl	2/cyl and	2/cyl and	2/cyl	2/cyl	2/cyl
364	3/cube		joint	joint			

BHL - 1:3 **Testing at Standard State** (assumed 28 days)

Age	Compressive Strength C 109 (determines Standard State) *Quant/ Type*	Elastic Mod. Dynamic Modulus ASTM E1875 *Quant/ Type*	**WVT** ASTM E 96 *Quant/ Type*	E 96 Modified W/ Isopropyl *Quant/ Type*	Leeds - Air Perm Cell *Quant/ Type*	Poroscope *Quant/ Type*	Falling Head Permeameter ASTM D5856-95(2002)e1 *Quant/ Type*
7	3/cube						
14	3/cube						
28	3/cube	3/cyl	2/cyl and joint	2/cyl and joint	2/cyl	2/cyl	2/cyl
56	3/cube						
84	3/cube						

[1] Alshamsi, Abdullah, Imran, Hassan, "Development of a Permeability Apparatus for Concrete and Mortar." *Cement and Concrete Research* **32** (2002) 923-929.
[2] Hearn, N. *"Comparison of Water and Propan-2-ol Permeability in Mortar Specimens."* Advances in Cement Research **8** No. 30 *(1996).*
[3] *Loosveldt, Helene, Zoubeir Lafhaj, Frederic Skoczylas. "Experimental Study of Gas and Liquid Permeability of a Mortar."* Cement and Concrete Research **32** *(2002) 1357-1363.*

APPENDIX III
COMPRESSION TEST RESULTS

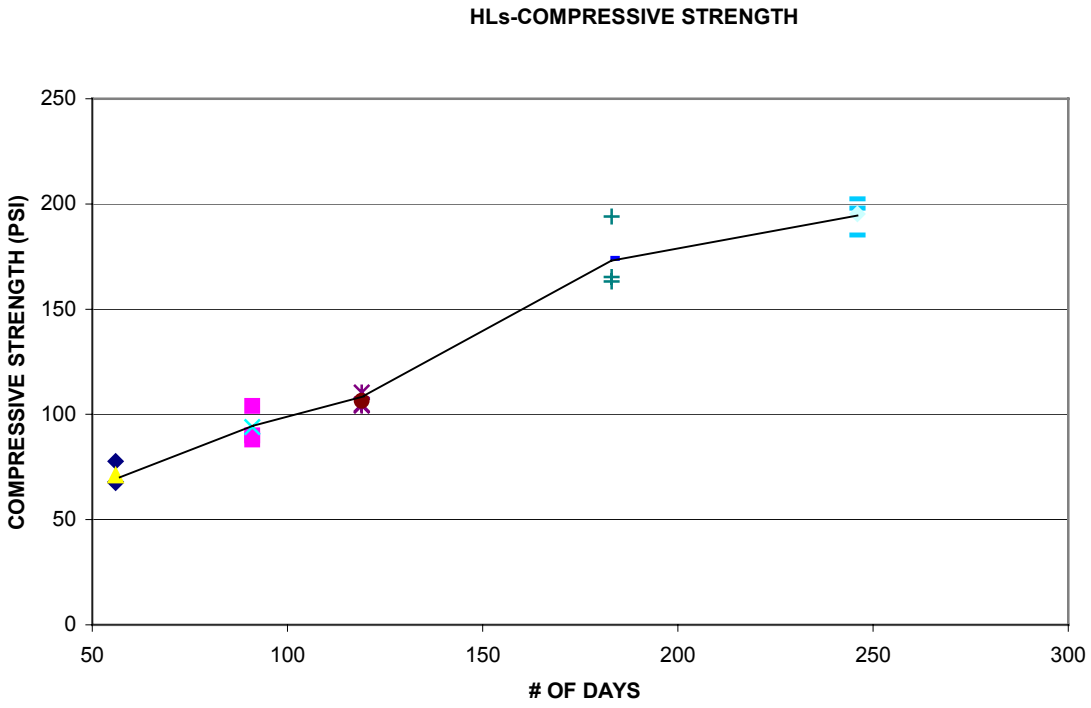
HLs-COMPRESSIVE STRENGTH
COMPRESSIVE STRENGTH (PSI)
250
200
150
100
50
0
50
100
150
200
250
300
OF DAYS

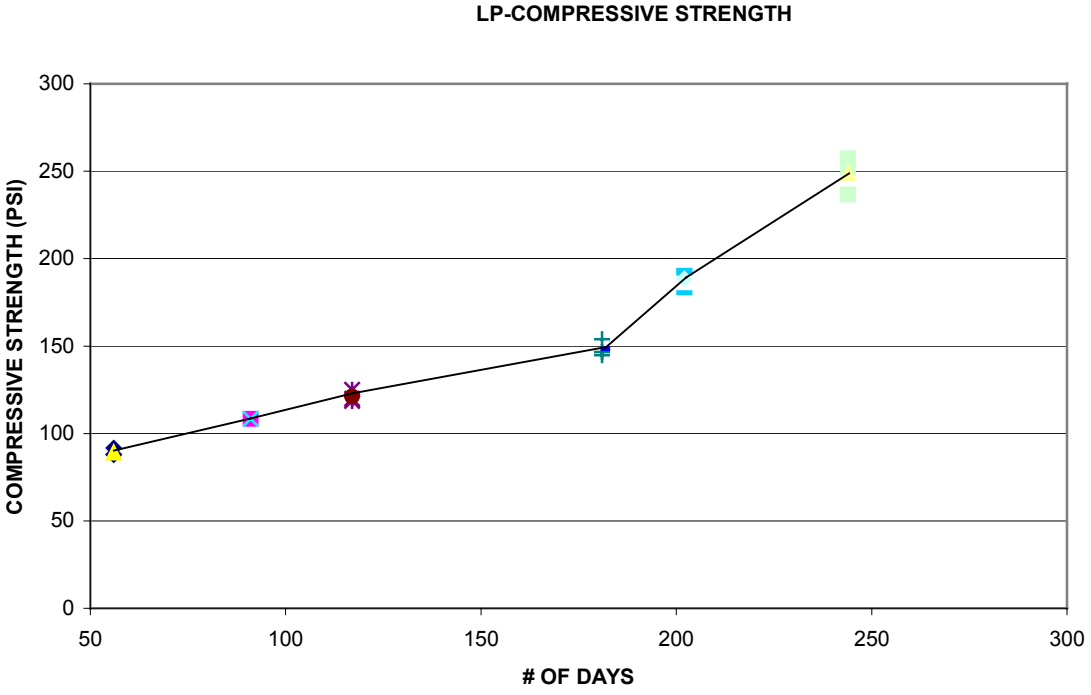
LP-COMPRESSIVE STRENGTH
COMPRESSIVE STRENGTH (PSI)
300
250
200
150
100
50
0
50
100
150
200
250
300
OF DAYS

HHL1-COMPRESSIVE STRENGTH

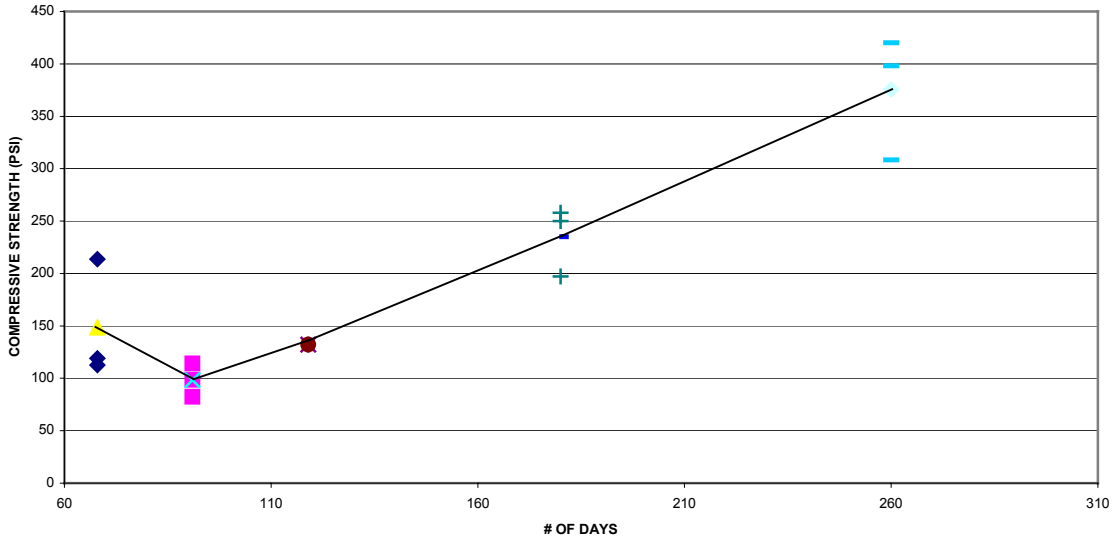

HHL2-COMPRESSIVE STRENGTH

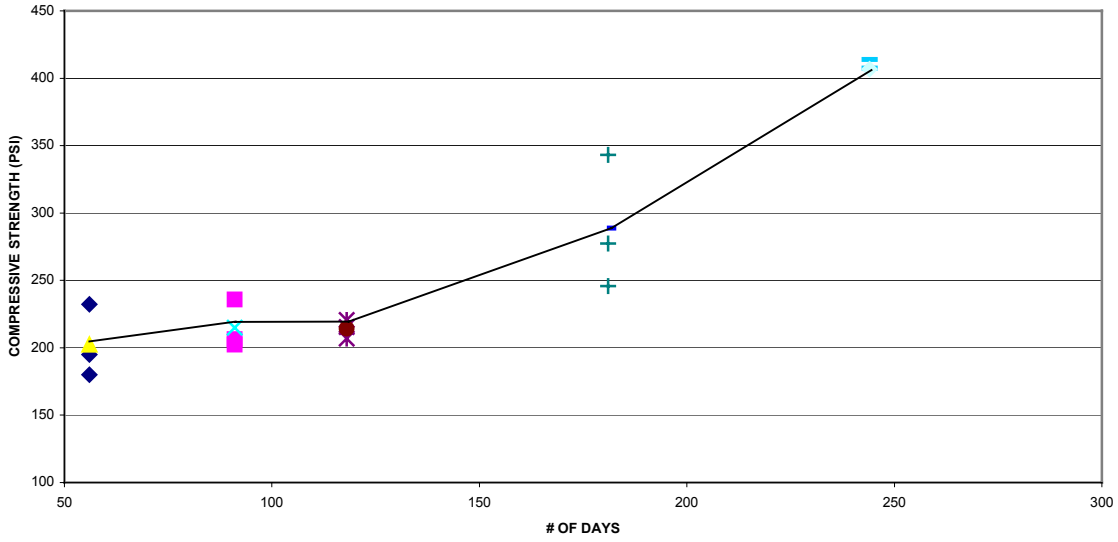

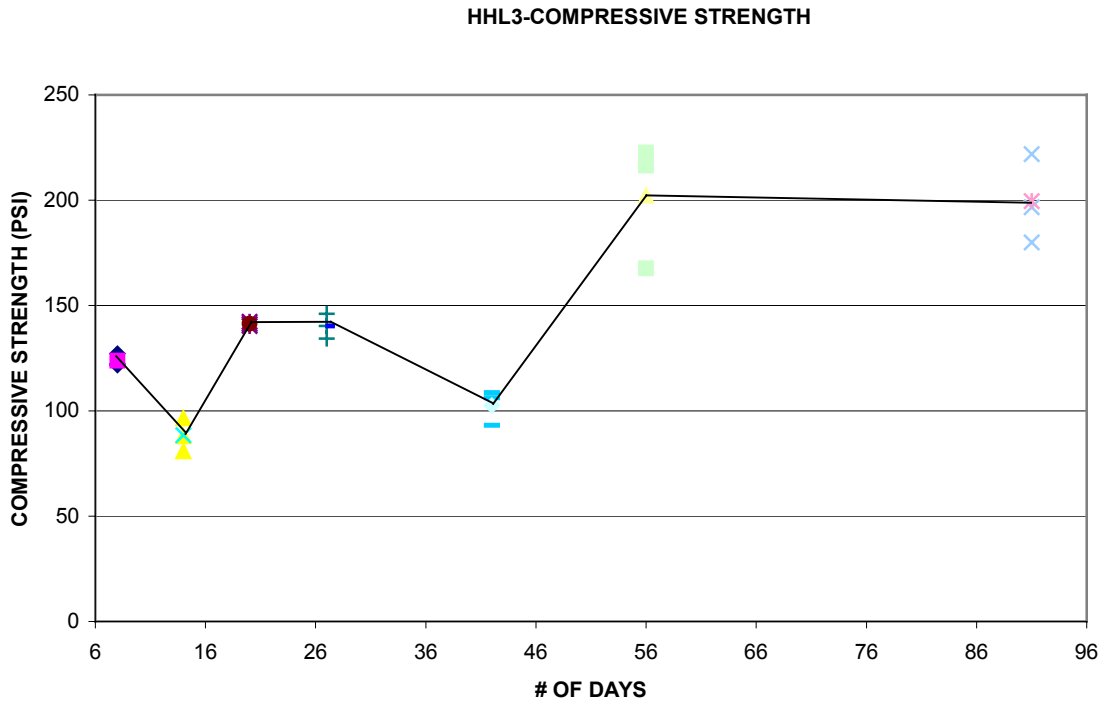
HHL3-COMPRESSIVE STRENGTH
COMPRESSIVE STRENGTH (PSI)
250
200
150
100
50
0
6
16
26
36
46
56
66
76
86
96
OF DAYS

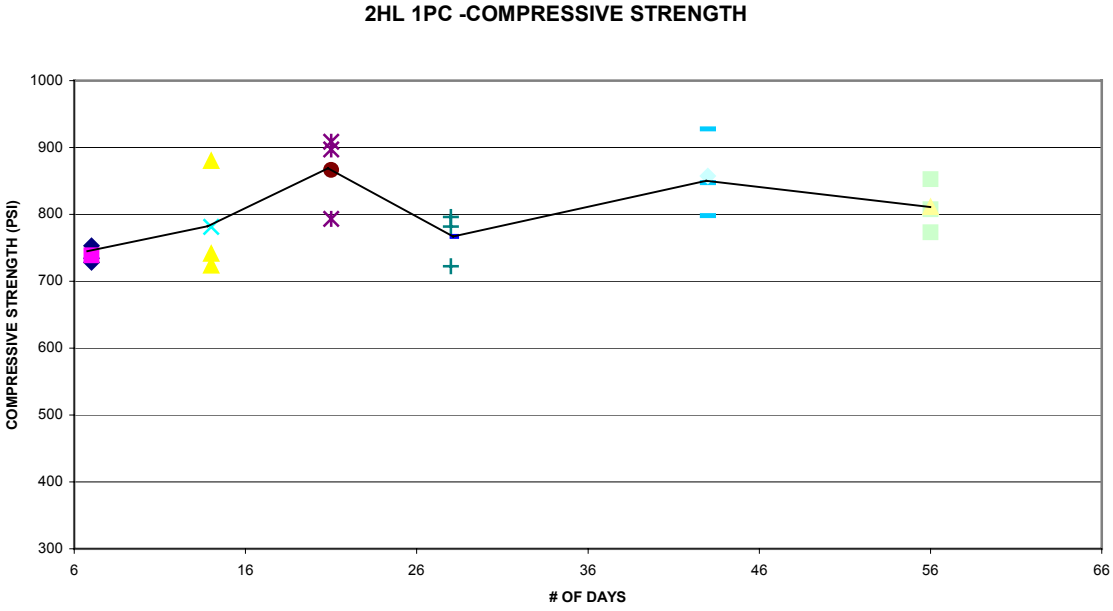
2HL 1PC -COMPRESSIVE STRENGTH
COMPRESSIVE STRENGTH (PSI)
1000
900
800
700
600
500
400
300
6
16
26
36
46
56
66
OF DAYS

3HLs:1 PC-COMPRESSIVE STRENGTH

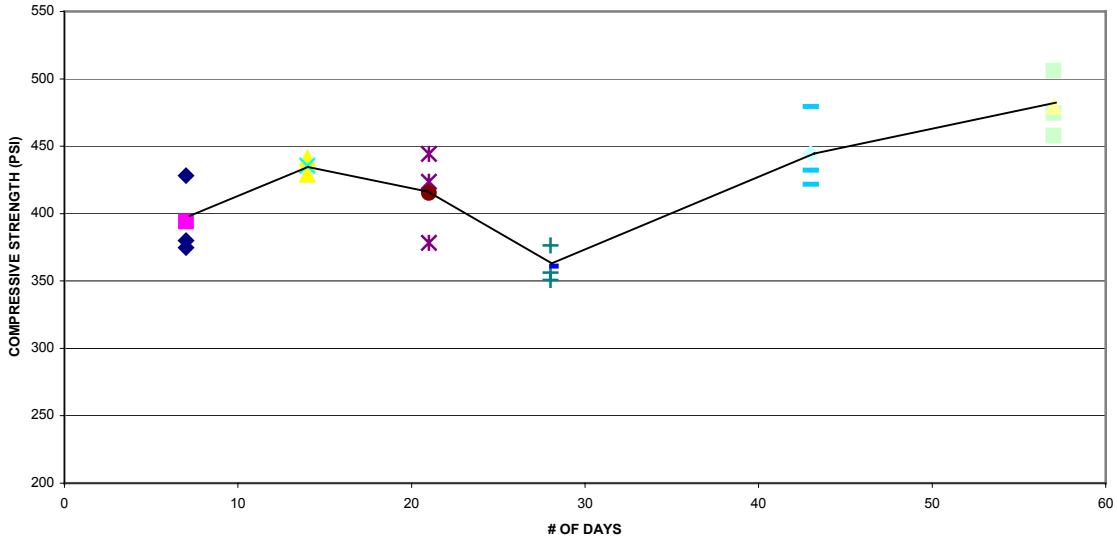

Time vs. Compressive Strength

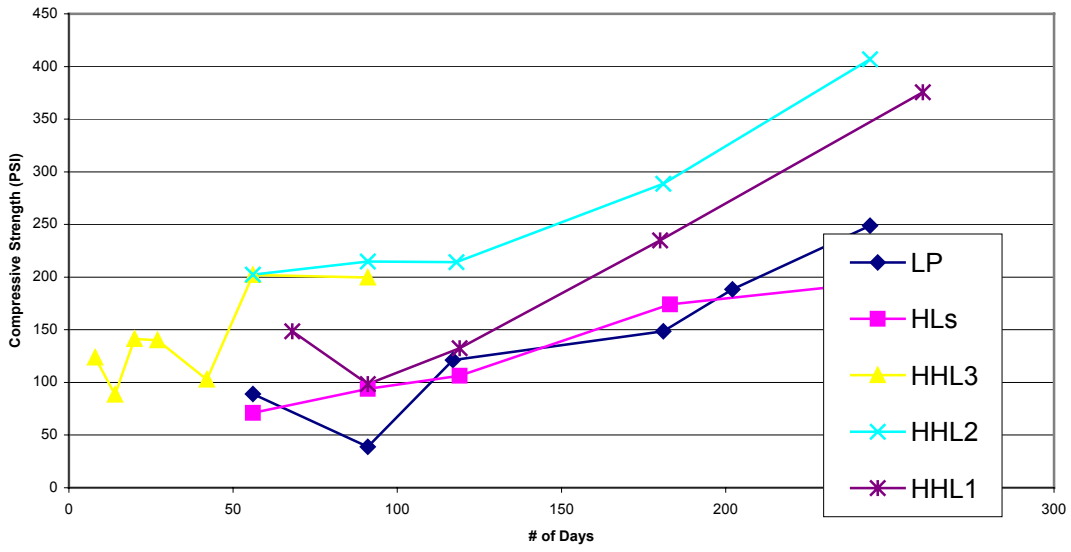

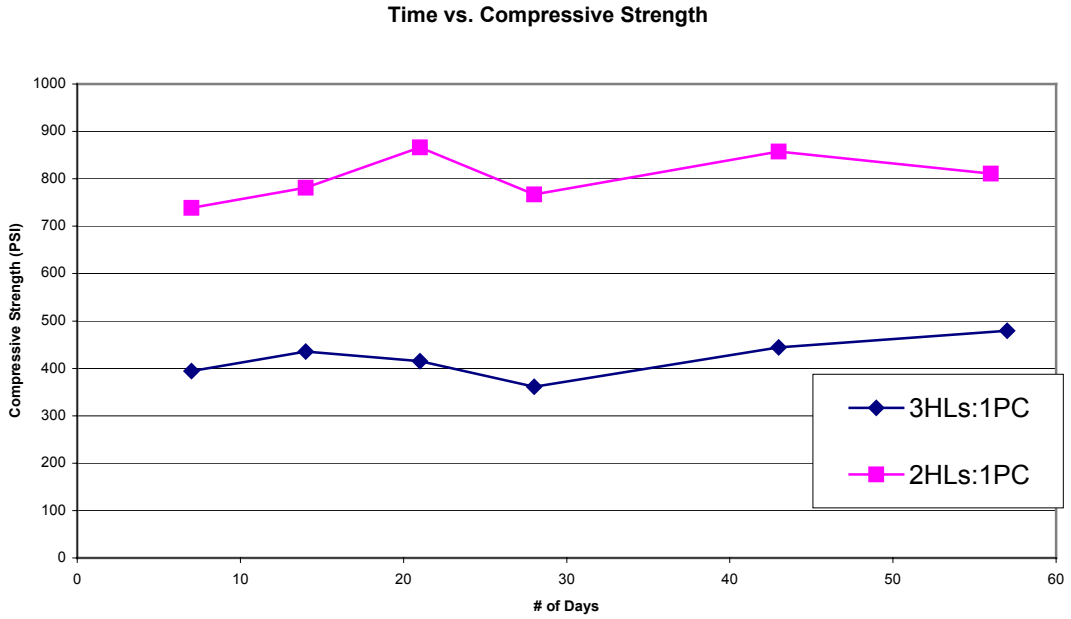
Time vs. Compressive Strength
Compressive Strength (PSI)
1000
900
800
700
600
500
400
300
200
100
0
0
10
20
30
40
50
60
# of Days
3HLs:1PC
2HLs:1PC

APPENDIX IV
DYNAMIC YOUNG'S MODULUS OF ELASTICITY FOR MASONRY MORTARS

Job Name: NCPTT
Job #: 04-084
Atkinson-Noland & Associates
Author: Matthew McNeil
September 1, 2005

Dynamic Young's Modulus of Elasticity for Masonry Mortars

I. Purpose/Scope:

The purpose of this test was to non-destructively determine the Young's Modulus of Elasticity of masonry mortars. The general testing method is in accordance with ASTM C 215-97, *Standard Test Method for Fundamental Transverse, Longitudinal, and Torsional Resonant Frequencies of Concrete Specimens* **[1]**. ASTM C 215 essentially explains an approach for measuring Young's Modulus dynamically by exciting a specimen and determining the specimen's resonant frequency.

II. Equipment:

The determination of the resonant frequency followed the 'Forced Resonance Method' explained by ASTM C215-97 for measuring transverse frequency; therefore, all components explained below were chosen in an attempt to follow this standard.

Sensor (accelerometer):

-Manufacturer: PCB Piezotronics
-Model: 356A02 (Triaxial accelerometer)
-Sensitivity: 10 mV/g
-Frequency Range: 1-5 KHz
-Measurement Range: +/- 500 g pk
-Weight: 0.37 oz (10.5gm)

Signal Conditioner:

-Manufacturer: PCB Piezotronics

-Model: 481A02 SN 230

Filter Module:

-University of Colorado (ITLL)

SCXI-1141

Data Acquisition:

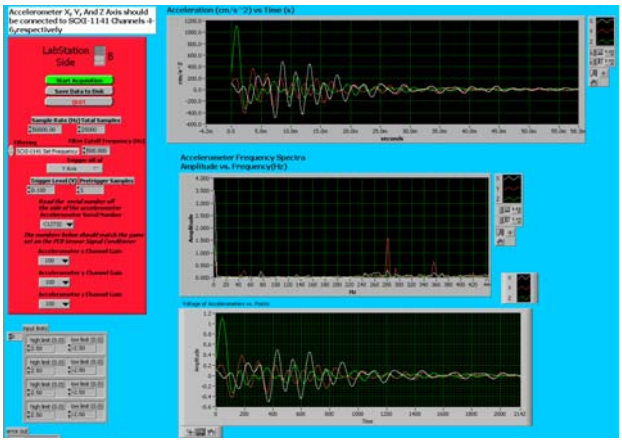

-LabView 7.1 (Graphical Development Software for testing and Measurement)

-University of Colorado (ITLL) Module: 'PCB Triaxial Accelerometer.vi'

Mounts:

-Accelerometer: Threaded nut mounted with duct tape (to protect sample) and hot melt glue.

-Sample: Two 6 inch pieces of angle aluminum (L1.5x1.5x1/4), with sharpened edges to stay within node lines more effectively.

Impactor:

-Ballpoint pen insert (flexible polymer rod) with small nut on end (Diameter = 0.365 inch, Mass = 1.39 g; including weight of glue). Mounted in clamp to ensure consistent striking location, and impact force. Note: In order not to damage the mortar specimens, a lighter weight head was used; therefore, the impactor does not follow ASTM specifications.

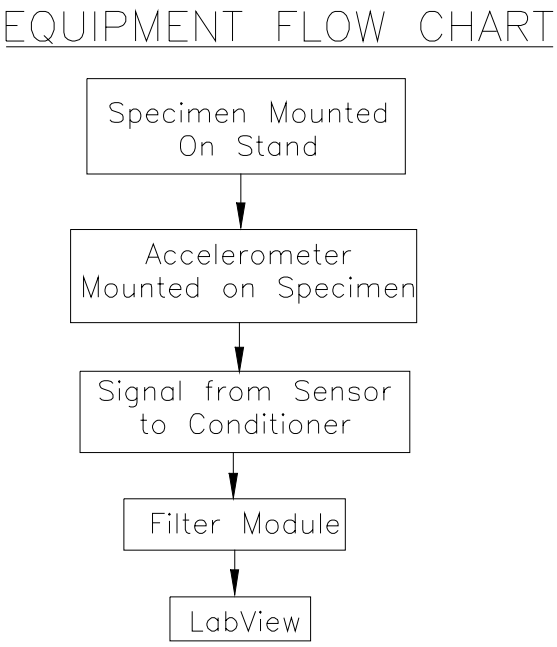

Diagram-1: Equipment Flow Chart

III. Test Setup

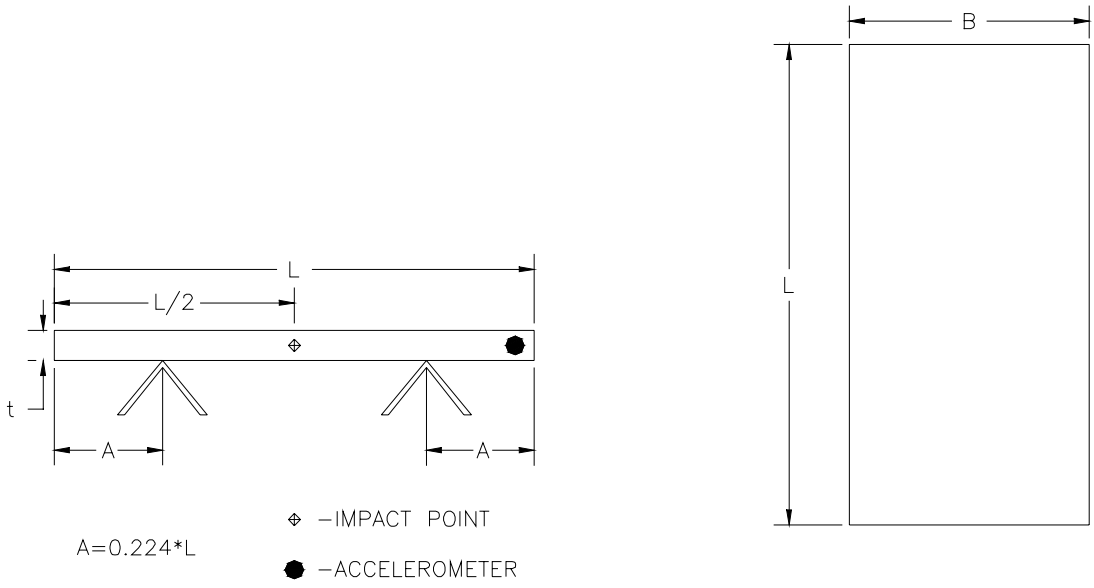

Diagram-2: General Test Setup and Geometric properties explanation

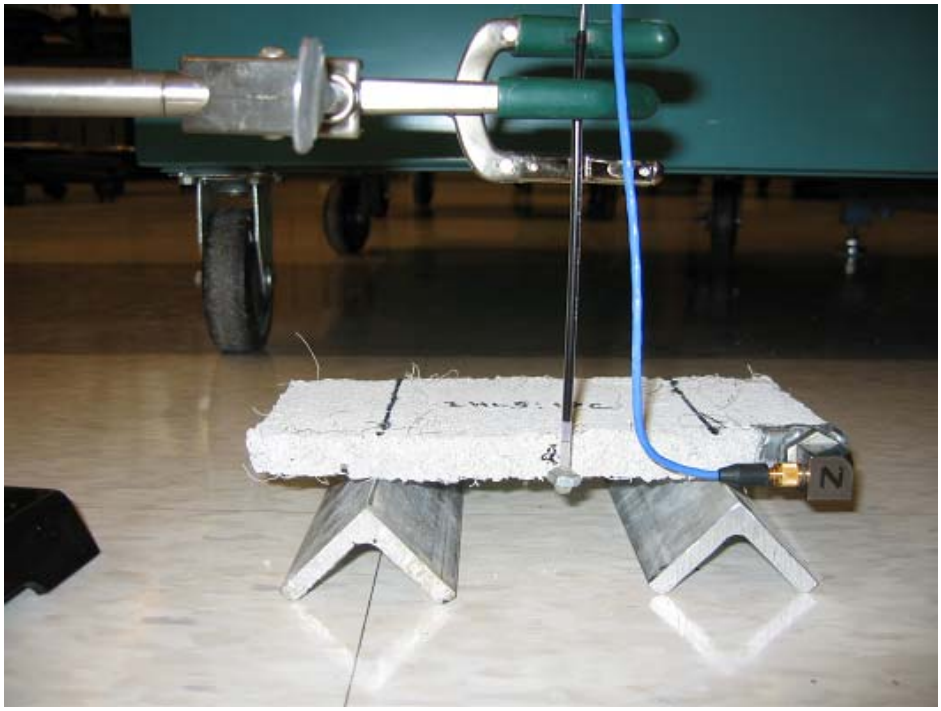

Photo-1: Overall Test Setup Showing support system, impactor, and accelerometer

IV. Procedure/ Process Description

The first step for setting up the experiment was to reprogram the LabView Visual Interface (VI). The current VI did not contain any filtering or windows, therefore, Hanning Windows were implemented on all outputs, and a low-pass filtering option was developed. The next step was to determine all parameters, including: necessary external gain, maximum voltage (to fit within system filter module requirement of 6 Vpp_max), sampling rate, total number of samples, and pre-triggering settings.

The following are the most significant parameters determined:

-Input Limits: +/- 2.5V

-Channel Gain: X100 (set on Signal Conditioner and in LabView)

-Trigger Level: 0.100V (with 1 pre-trigger sample)

-Filtering: SCXI-1141 Set Frequency w/ Filter Cutoff Frequency at 500 Hz

-Sample Rate: 50,000 Hz

-Total Number of Samples: 25,000 samples

-Calculation Overview:

The calculation for the dynamic Young's modulus of elasticity, E, in Pascals (Newtons per square meter) from the fundamental transverse frequency, mass, and dimensions of the test specimen is as follows:

$$Dynamic\ E = CMn^2$$

Where,

M = mass of specimen, kg;

n = fundamental transverse frequency, Hz;

C = $0.9464 \cdot (L^3T/B \cdot t^4)$, $N \cdot s^2/(kg \cdot m^2)$, for a prism;

L = length of specimen, m;

t, B = dimensions of cross section of prism, m;

T = a correction factor which depends on the ratio of the radius of gyration, K (K = t/3.464), to the length of the specimen, L, and on Poisson's ratio.

-System Verification:

Once the system seemed to be functioning properly, a steel rod (with a known Modulus of Elasticity) was tested to ensure proper test setup. The results were reasonable with a resolvable resonant frequency that provided a Modulus of Elasticity within 13% of the actual value **[2]** (see Diagram-2). This exercise was a good example of the 'fishing' for the correct resonant frequency from the Fast Fourier Transform (FFT). In other words, when the correct Modulus is known, the appropriate frequency range is predetermined, therefore, it was trivial to determine exactly where the correct frequency was located. Unfortunately, for the actual mortar specimens, the Modulus was unknown going into the experiment; therefore, the correct frequency range was unknown and more 'fishing' for values took place.

Frequency			Dynamic	Published	
Measured (Hz)	Goal (Hz)	Error (%)	Modulus (GPa)	Modulus (GPa)	Error (%)
18.6	19.9	6.5	175	200	12.7

Diagram-3: Results of Steel Rod for System Verification

-General Testing Procedure:

1. Take geometric measurements
2. Mark nodal lines and impact zone
3. Mount sensor
4. Weigh Specimen
5. Boot System
6. Press 'Start Acquisition' in LabView
7. Pull back and release impactor onto impact zone (middle of cross-section along plane of accelerometer)
8. Briefly view data for 'anomalies'
9. Save data
10. Repeat steps 6-9, 3 times
11. Move impactor to the node along same edge as before (far node from accelerometer) to 'truth' test *

12. Repeat steps 6-9, 3 times
13. Analyze data, by comparing the FFT of both center impact and nodal impact to determine the resonant frequency (Using Microsoft Excel)
14. Enter appropriate data into spreadsheet to calculate Young's Modulus

*In order to 'truth' test the measured resonant frequency from the FFT, the test is run by striking the specimen at the node, since in theory, the specimen will not resonate at it's natural frequency when impacted along a node. This provides a means of determining what is noise, or other resonant modes, and what is the actual natural resonant frequency.

V. Results

Two specimen types were tested and analyzed, HHL2 (Hydrated Hydraulic Lime-NHL3.5), and 2HLS:1PC (2 parts Hydrated Lime type S, 1 part Portland Cement) according to ASTM C 215. Both specimens were cast mortar joints approximately measuring 3.5 in x 8 in x 0.5 in. The results are as follows:

HHL2:

The following is a plot of the FFT for HHL2 taken from one run:

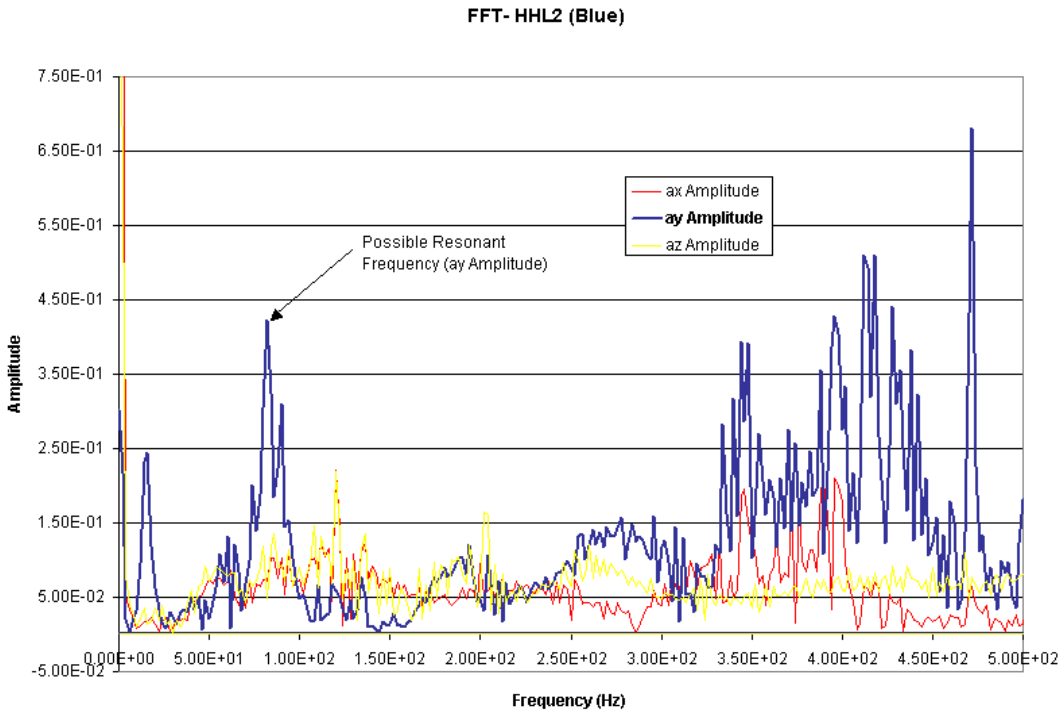

Diagram-4: FFT of HHL2, where ay line is the frequency of interest (based on the accelerometer orientation). **

**Often times, all three directions of acceleration were plotted in order to filter out certain noise elements. For example, any spikes that had all three lines in phase were often neglected.

The first predominant peak is at 14 Hz, however, this frequency was ignored, since it was observed on both specimen types and even on some of the nodal impact FFTs. The next spike occurs at around 82 Hz; therefore, in order to determine if this is actually the natural frequency, the specimen must be 'truthed' by impacting it along the nodal plane. Below is a plot of the FFT for the same specimen, this time impacted at the nodal plane:

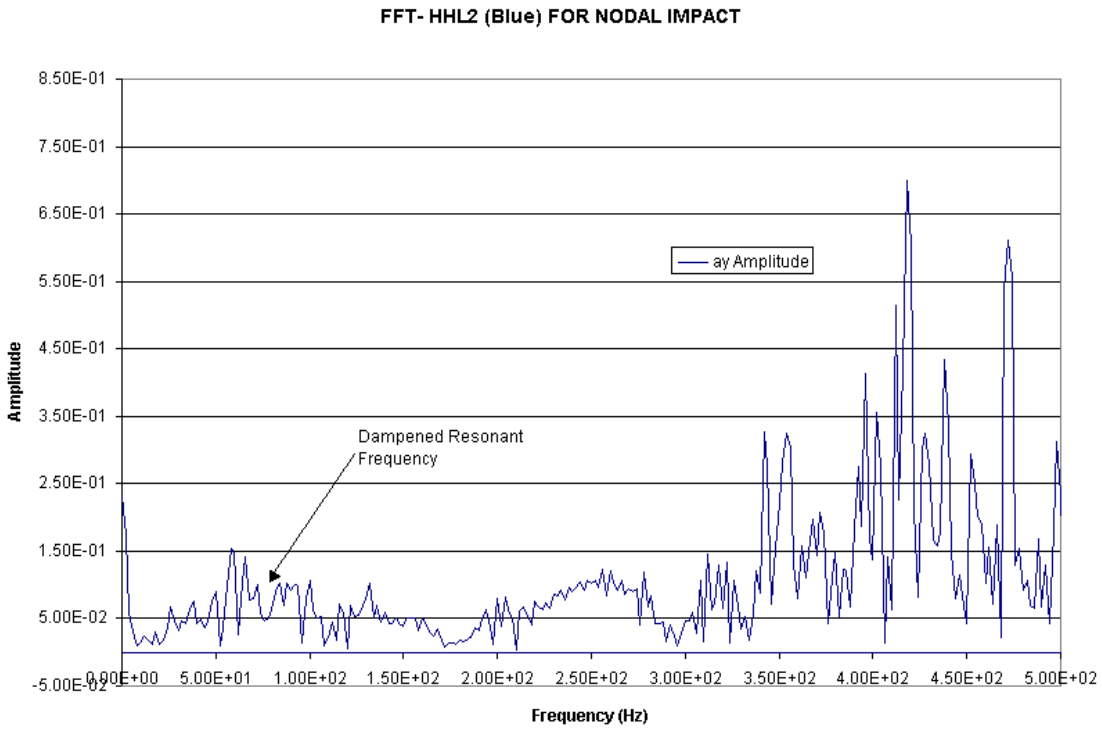

Diagram-5: FFT of Nodal Impact data for HHL2

As expected the natural frequency previously measured at a frequency of ~82Hz is no longer a predominate spike, whereas some of the other spikes further down the spectrum are still observable.

The average frequency and modulus values will be presented below in a comparison with the HHL2 sample and the 2HLS:1PC.

2HLS:1PC:

Below is a plot of the FFT for 2HLS:1PC, which due to its Portland cement content, should be stiffer than the Natural Hydraulic Lime based HHL2.

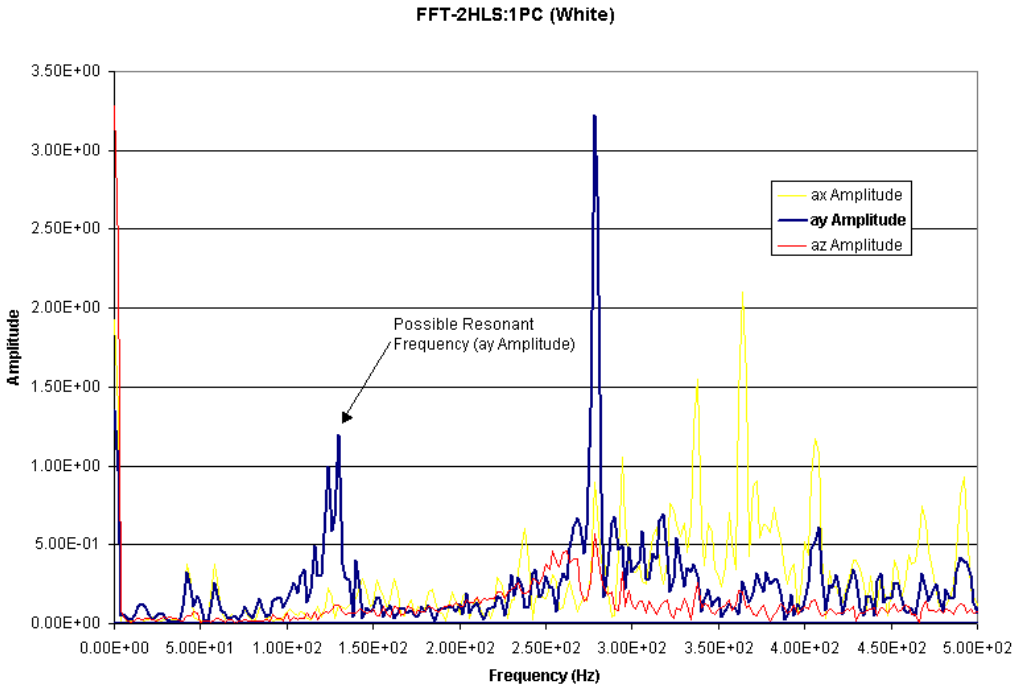

Diagram-6: FFT of 2HLS:1PC, where ay line is the frequency of interest (based on the accelerometer orientation).

Notice that the predominate spike, occurring around 278Hz, has all three accelerations showing the same pattern, therefore, this frequency is ignored. The only other intuitive frequency occurs around 124Hz. In order to justify this as the natural resonant frequency, the sample must be 'truth' tested similar to the HHL2 sample. The FFT from the nodal impact 'truth' test follows:

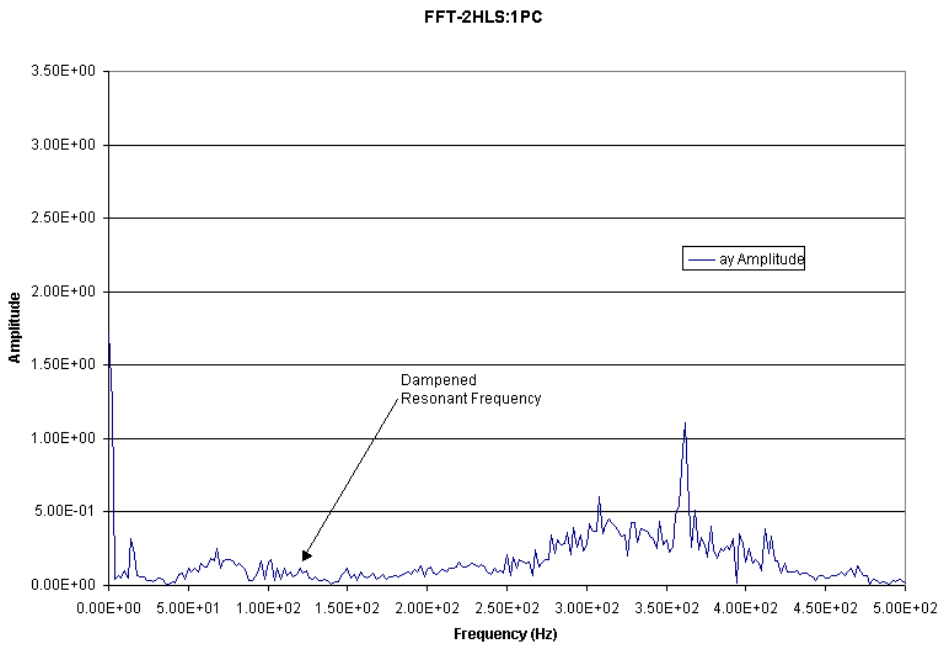

Diagram-7: FFT of Nodal Impact data for 2HLS:1PC

Notice that the assumed natural frequency seems to disappear in the 124 Hz range, therefore, this is most likely the natural resonant frequency of interest. Also, it is important to note that the 14 Hz peak that was observed in the HHL2 testing has returned, even for nodal impact, which is why it should be ignored for all testing.

The average frequency and modulus values are presented below in a comparison with the HHL2 sample and the 2HLS:1PC.

Dynamic Young's Modulus Results

	Resonant Frequency			Dynamic Young's Modulus	
Specimen	**Avg. Freq. (Hz)**	**StDev(Hz)**	**COV%**	**E (Gpa)**	**E (Kpsi)**
HHL2	83.0	1.4	1.7	0.31	45.5
2HLS:1PC	122.7	14.5	11.8	0.72	103.8

***

***It is important to mention that the coefficient of variation (COV%) for the two specimens is somewhat misleading, since there was not enough data taken on either of the specimens, especially the HHL2. In fact, it was much easier to resolve a resonant frequency for the 2HLS:1PC than it was for the HHL2. [See Appendix A for all data]

Therefore, the final results are as expected since the Portland based 2HLS:1PC sample has a higher Young's Modulus (stiffer) than the HHL2 specimen.

VI. Conclusions/ Recommendations

In conclusion, a testing method was followed to determine the Dynamic Modulus of Elasticity according to ASTM C 215-97. Overall, the testing apparatus and system seem to be functioning properly, as was shown with the testing of the steel bar with a known Modulus. Unfortunately, the system is not as capable when testing the mortars, most likely for a variety of reasons.

The first possible source of error is that the geometry of the bed joint specimens barely fit within the ASTM specification, in that the width, B, was too large for the length, L. A more desirable shape would be a long slender cylinder or bar.

Additionally, more error could be a consequence of not knowing the values of Poisson's ratio for the mortars. This is because the calculation for the Dynamic Modulus of elasticity was based on a value for Poisson's ratio. Since Poisson's ratio was unknown, an estimated value of 0.3 was used. The fact that Poisson's ratio is unknown could certainly influence the results, not only because this value was assumed, but also since the correction factor that uses Poisson's ratio did not have data for values above 0.26 (the correction value used for the calculations was extrapolated for a Poisson's Ratio of 0.3).

Other possible sources of error include: the inexact geometry of the bed joint and its impact on the placement of the nodal supports, non-homogenous test specimens, the weight of the sensor cantilevered over the specimen, and the cord of the accelerometer restricting some differential movement and acceleration. Moreover, it is impractical to

measure specimens from the field; therefore, the comparison is limited to specimens cast in the lab. All of these issues most likely influenced the results in some way and added to the difficulty experienced when attempting to pick out a single definite natural resonant frequency.

It is also important to mention that the data presented above should not be interpreted with high confidence since only one specimen of each type was measured only a handful of times.

There are several future recommendations for applying this testing method to low stiffness mortar specimens. First of all, a study should be conducted to determine the effects of the geometry of the specimen, by casting various other shapes of the same material. Also, a study concerning the effects of Poisson's ratio should be conducted, as well as perhaps iteratively calculating a more precise Poisson's ratio. It would also be helpful to cast a cementitious specimen with a known modulus of the same geometry to further ensure proper system setup and calibration. (Verify through mechanical tests-elastic modulus).

Above all, there needs to be much more data taken for each specimen once most of the other factors of error are dealt with, in order to create a better global population for error and uncertainty analysis. If the averaging of several impacts could be implemented before any computational method is performed, the results could reflect less error. In other words, it is likely that if the time domain data for 5 impacts could be averaged before the FFT, the results should be clearer with less noise. Also, when having to collect a greater number of data points, it would be favorable to create a more automated method of taking the data from LabView (both the center impact and the nodal) and having the natural resonant frequency outputted automatically.

In summary, the testing method for calculating the Dynamic Young's Modulus of Elasticity is not difficult to conduct, however, it can be difficult to interpret the results, most likely due to the several factors mentioned above. Currently there is a working system for performing this test, although, at this point several factors of variance should be investigated before a catalog of values for masonry mortars is produced.

Summary of Observations/ Recommendations:

- Geometry of bed joint specimen is unfavorable; it would be more appropriate to have a long slender bar with a ratio of length to maximum transverse direction between 3 and 5.
- Specimens must be handled with care due to their fragility, since any type of fracture or flaw could influence the results considerably.
- The experiment requires a lightweight accelerometer of negligible weight when compared to the specimen.
- The resonant frequency of the accelerometer must be at least twice the maximum operating frequency.
- While a uni-axial accelerometer is sufficient for the required frequency measurement, a tri-axial accelerometer is beneficial in separating noise from the signal of interest.
- It appears important to take care in having a uniform shaped specimen, such that the nodal lines are easy to define and are accurate. Furthermore, the nodal supports must be designed with sharp edges to minimize nodal overhang.
- The impactor seems to work better with a flexible shaft. Moreover, care must be taken not to damage the fragile specimens during impact.
- Even though it is not required, it may be desirable to be consistent with the way the specimen is impacted, maintaining a constant force and location.
- An accurate known Poisson's ratio is desirable for calculations.
- Averaging several impacts at once before determining frequency is desirable to minimize noise in the FFT output.
- Care must be given with the mounting of the accelerometer, to ensure no damage to specimen, and so that the connecting wires do not impede movement.
- An automated procedure for extracting the resonant frequency from LabView would be desirable.
- Determining the natural resonant frequency becomes trivial if the expected value is known a head of time, such as with a material with a known modulus.

VII. References

[1] ASTM C 215-97. Standard Test Method for Fundamental Transverse, Longitudinal, and Torsional Resonant Frequencies of Concrete Specimens. 1998. ASTM International

[2] http://www.matweb.com/search/SpecificMaterial.asp?bassnum=MSA36A. "ASTM A36 Steel, Bar". Accessed 8/4/2005.

HHL2- DATA SHEET AND PLOTS

Job Name NCPTT
Job # 04-084

Date 8/25/2005
By MGM

Dynamic Young's Modulus
(via the Fundamental Transverse Resonant Frequency)
(ASTM C215)

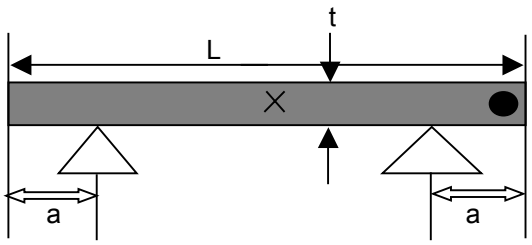

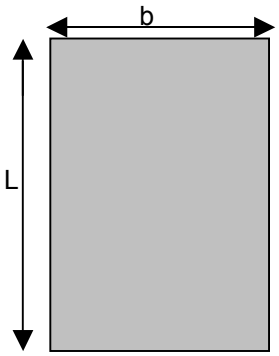

a=0.224*L

●-Accelerometer
╳-Impact Point

SAMPLE NAME: HHL2 (BLUE #1)

PROPERTIES:

Mass	m	0.4595	kg
Width	b	0.095	m
Length	L	0.2	m
Thickness	t	0.013	m

CORRECTION FACTOR: f(K/L, Poisson's Ratio)

Radius of Gyration: K= b/3.464; Poisson's Ratio: v

v	0.3
K/L	0.14
T	2.43

FUNDAMENTAL TRANSVERSE RESONANT FREQUENCY:

	Trial #1*	Trial #2*	Trial #3*		Average(Hz)	StDev(Hz)	COV(%)
n	82	84		Hz	83.0	1.4	1.7

DYNAMIC YOUNG'S MODULUS:

E=MCn^2

C=.9464(((L^3)*T)/(B*t^3)) {N*(s^2)*kg*m^2}

E	0.31	GPa
	45.5	Kpsi

-Anti-Nodal Impact for determining the natural resonant frequency:

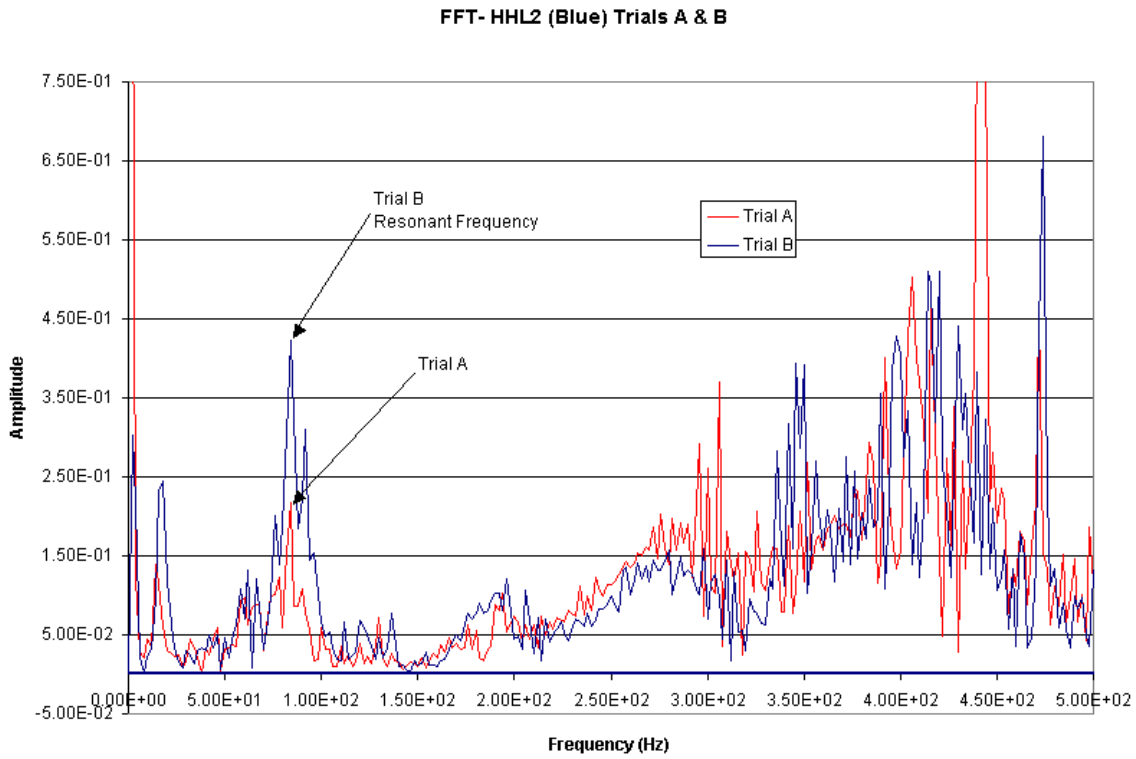

-Nodal impact for truth testing the resonant frequency:

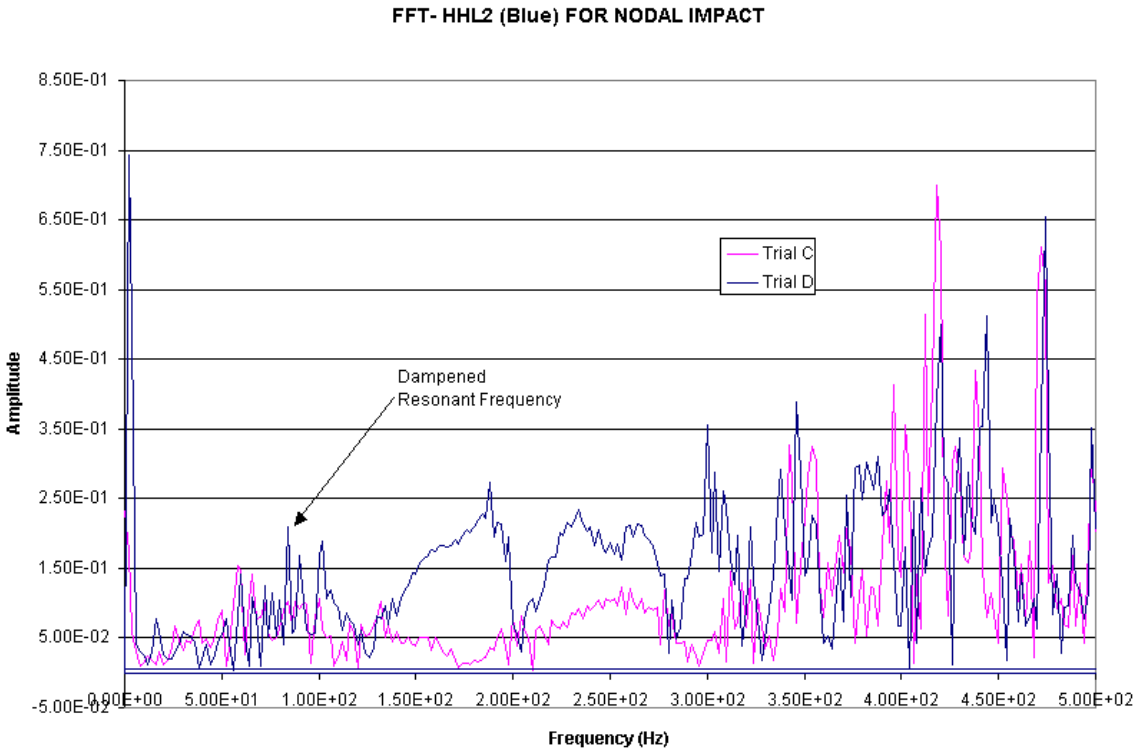

2HLS:1PC- DATA SHEET AND PLOTS

Job Name NCPTT
Job # 04-084

Date 8/31/2005
By MGM

Dynamic Young's Modulus
(via the Fundamental Transverse Resonant Frequency)
(ASTM C215)

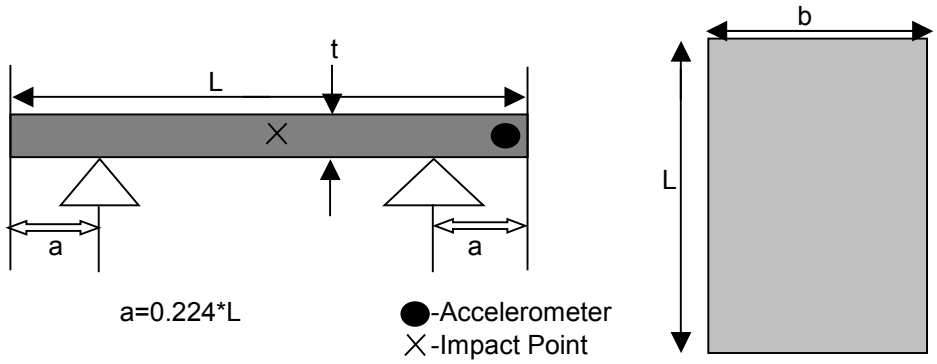

SAMPLE NAME: 2HLS:1PC (WHITE)

PROPERTIES:

Mass	m	0.4481	kg
Width	b	0.093	m
Length	L	0.195	m
Thickness	t	0.012	m

CORRECTION FACTOR: f(K/L, Poisson's Ratio)

Radius of Gyration: K= b/3.464; Poisson's Ratio: v

v	0.3
K/L	0.14
T	2.43

FUNDAMENTAL TRANSVERSE RESONANT FREQUENCY:

	Trial #1*	Trial #2*	Trial #3*		Average(Hz)	StDev(Hz)	COV(%)
n	106	130	132	Hz	122.7	14.5	11.8

DYNAMIC YOUNG'S MODULUS:

E=MCn^2

C=.9464(((L^3)*T)/(B*t^3)) {N*(s^2)*kg*m^2}

E	0.72	GPa
	103.8	Kpsi

-Anti-Nodal Impact for determining the natural resonant frequency:

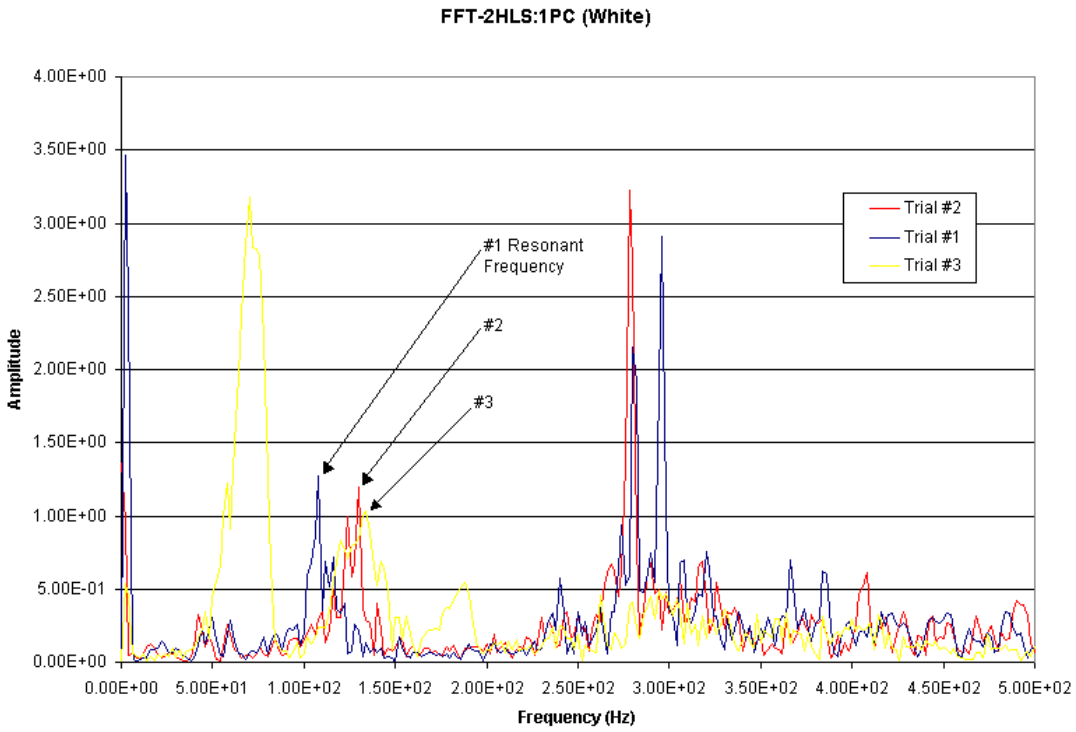

-Nodal impact for truth testing the resonant frequency:

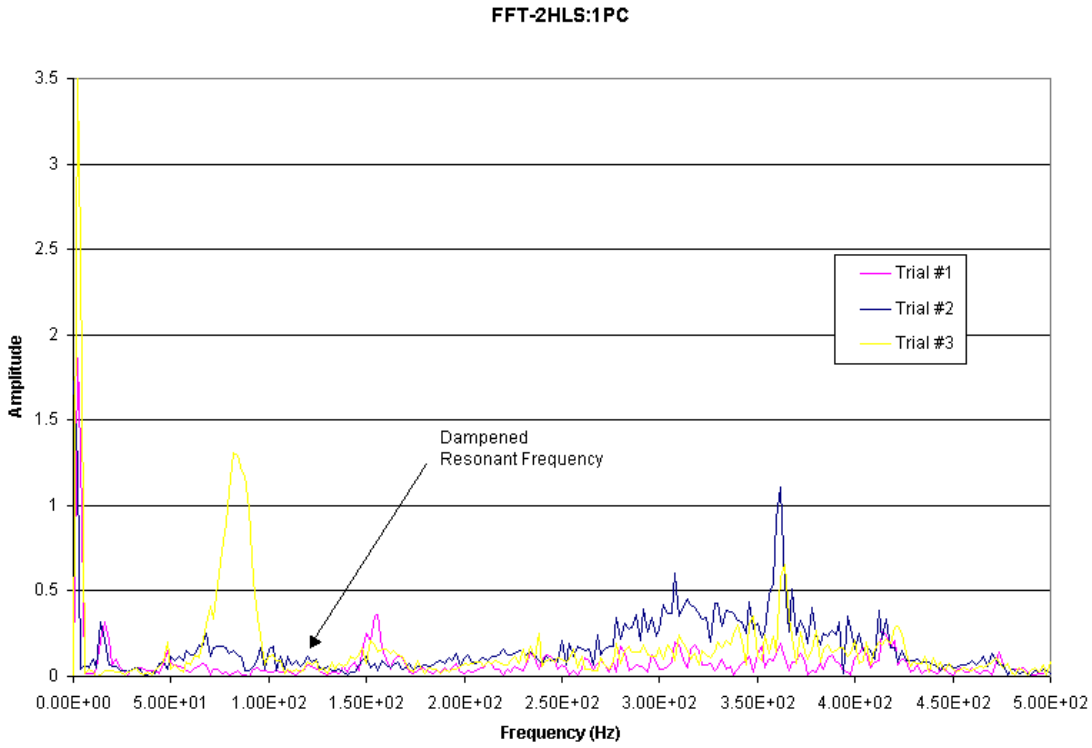

APPENDIX V
FINITE ELEMENT INVESTIGATION RELATING CARBONATION RATIO TO COMPRESSIVE STRENGTH FOR CAST MORTAR CUBES

Job Name: NCPTT
Job Number: 04-084
Atkinson-Noland and Associates
Author: Matthew McNeil
December 20th 2005

Finite Element Investigation
Relating Carbonation Ratio to Compressive Strength
For Cast Mortar Cubes

Objective:

The purpose of this investigation was to use finite element analysis to determine the effects of various carbonated shell thicknesses on compressive strength of cast mortar cubes. During the curing process of mortar, lime in the mix contributes to compressive strength as it carbonates. Lime carbonation proceeds from the outside cube surface inwards, resulting in creation of a high strength shell over a lower strength (un-carbonated) core. Compression tests conducted during this curing process indicated that at certain test ages the measured compressive strength leveled off or even decreased (see Figure 6 for an example). Therefore, the following analysis was conducted in an effort to determine if the temporary halt in strength gain was possibly a result of the carbonated shell phenomenon.

Software:

The finite element analysis was conducted using ANSYS 9.0.

Modeling / Analysis Procedure:

The mortar cubes were modeled to represent situations encountered during compression tests. Two-inch cubes were modeled as a simple two-dimensional surface with a section of high strength steel on the top to evenly distribute the compressive load. Four total models were developed and analyzed to correspond to carbonated shell thicknesses of 1/4”, 3/8”, 1/2" and ¾ inch. For this model, the compression stiffness of the carbonated lime section was assumed to be approximately three times the compression stiffness of the un-carbonated lime section. The steps below describe the modeling and analysis procedure.

Material Properties

Type 1: High Strength Steel Block
Plane 183 (8 node) – plane stress with thickness (t=2”)
E = 2.97E10 psi[1]
v = 0.29

[1] Exaggerated modulus to simulate compression testing conditions and distribute load evenly

Type 2: High Strength Carbonated Mortar Shell

Plane 183 (8 node) – plane stress with thickness (t=2")
E = 1.27E6 psi [2]
v = 0.3

Type 3: Low Strength Non-Carbonated Mortar Core

Plane 183 (8 node) – plane stress with thickness (t=2)
E = 4.03E5 psi [3]
v = 0.3

Analysis

1. Set analysis type to 'Structural, h-method'
2. Defined 2D element type 'solid plane 183 – 8 node plane stress with thickness'
3. Created material models for all three material types and inputted material properties E, v
4. Modeled keypoints at every endpoint of every line
5. Created lines to connect all keypoints
6. Created areas for each material section between the lines
7. Free meshed each area individually
8. Manually changed material number for each element to correspond to the appropriate material type (either steel, carbonated shell or non-carbonated core)
9. Free meshed all areas
10. Refined mesh twice for all areas
11. Set boundary conditions: fixed bottom line of the mortar cube (set structural displacement equal to zero in all degrees of freedom)
12. Defined loads: applied unit pressure along top surface of the steel
13. Solved the model for current load step
14. Conducted contour plot of the Von Misses Stress
15. Listed and sorted the maximum Von Misses stress according to the element number and determined the element number within the mortar cube that experience the maximum amount of stress
16. Repeated analysis for four total shell thicknesses (1/4", 3/8", 1/2", 3/4")
17. Analyzed results

[2] Based on E =57,000*(fm')^(1/2); where fm' = 500 PSI (compressive strength estimation)

[3] Based on E =57,000*(fm')^(1/2); where fm' = 50 PSI (compressive strength estimation)

Results:

The following Figures show analysis results as contour plots of the Von Misses stress for each of the four models. The maximum stress for each case occurred near the interface of the shell and core approximately half way up the specimen (Note: Tabulated results for all models follow the visual results):

Quarter-Inch Shell:

Maximum Value =

471 2.0226

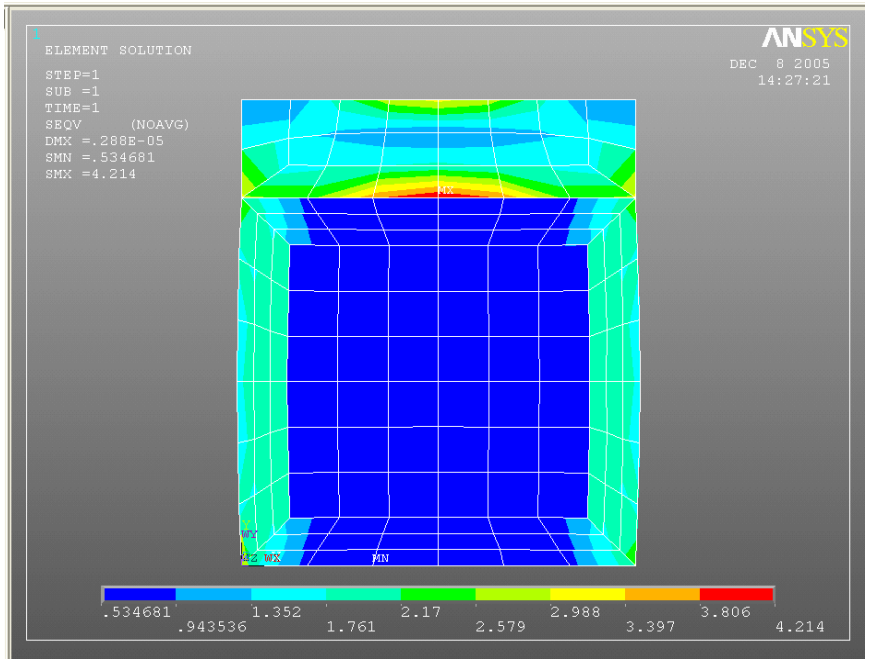

Figure 1: Quarter-Inch Shell Contour Plot

Three-Eighths Inch Shell:

Maximum Value =

953 1.8088

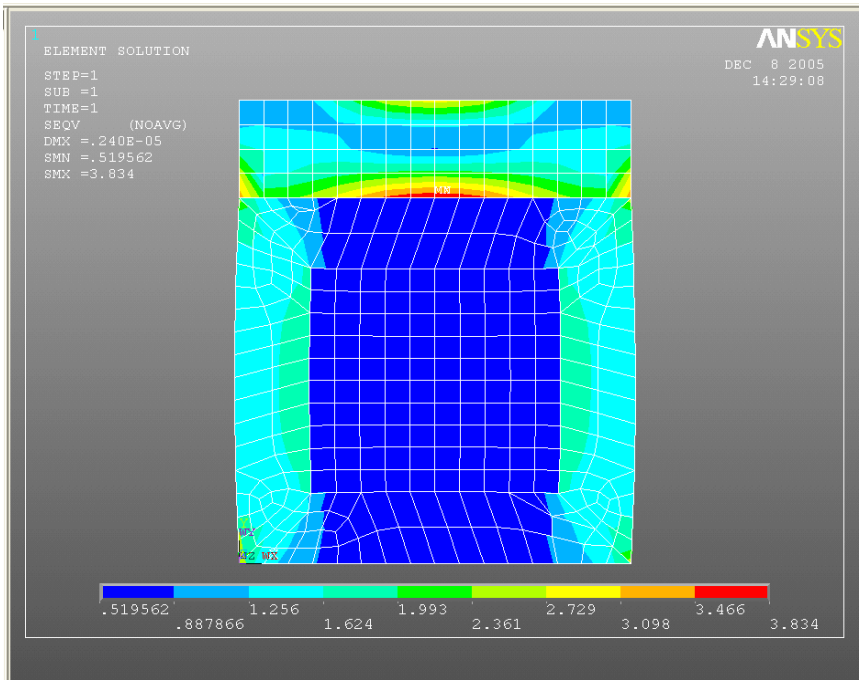

Figure 2: Three-Eighths Inch Contour Plot

Half Inch Shell:

Maximum Value =

1505 1.661

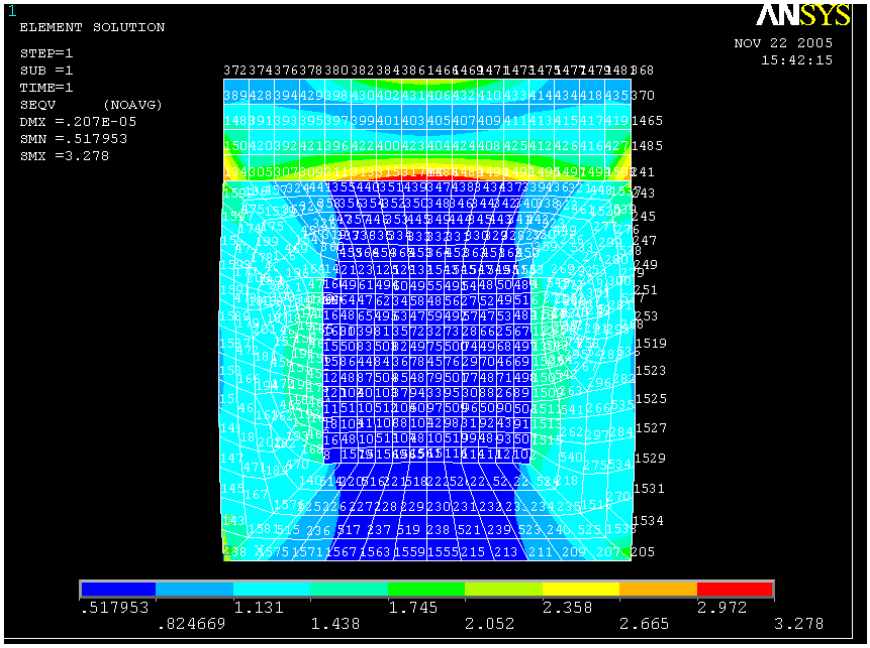

Figure 3: Half Inch Contour Plot

Three-Quarter Inch Shell:

Maximum Value =

185 1.4975

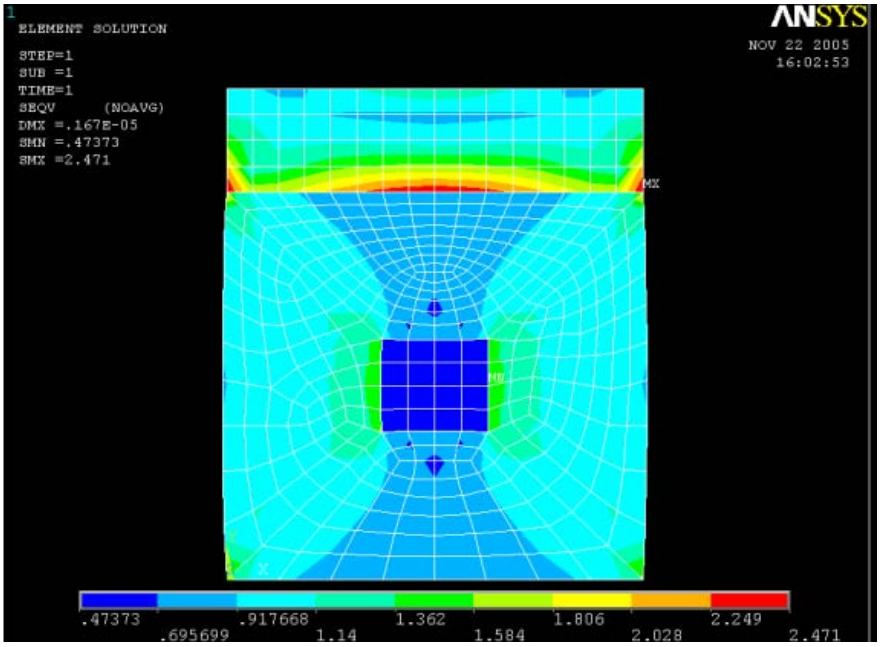

Figure 4: Three-Quarter Inch Contour Plot

Table 1 lists results of the finite element analysis for all four models including the values for the maximum load experienced due to the applied unit load (Max Load), the equivalent load for actual failure (sigma), and the dimensionless load ratio of sigma divided by the maximum 500 psi strength (sigma/sigma_max).

Table 1: *Tabulated Final Results*

	No Shell	1/4	3/8	1/2	3/4	All Shell
Max Load (unit)		2.0226	1.8088	1.661	1.4975	
Sigma	50	247.2	276.4	301.0	333.9	500
sigma/sigma_max	0.1	0.49	0.55	0.60	0.67	1

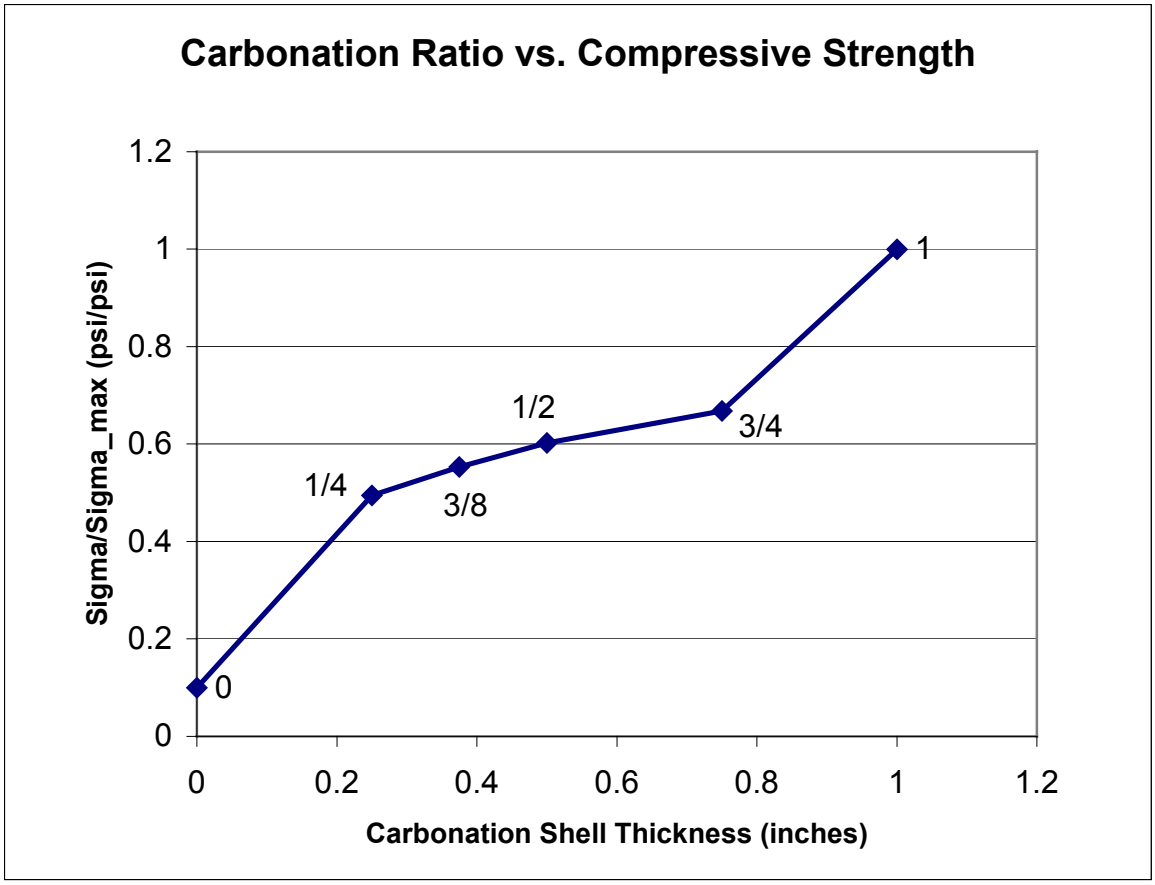

Figure 5: Carbonation Ratio vs. Compressive Strength for all models

Figure 5 shows that the rate of compressive strength gain appears to decrease during the curing period when the carbonated shell propagates through the specimen. For the purpose of this study, the point at which the cubes gain 75 percent of their ultimate strength is defined as "standard state". Based on results of this analysis, the specimen will be carbonated through approximately 80 percent of the cube dimension at standard state.

Conclusions:

In summary, an attempt was made to investigate the effects of the relative carbonated shell thickness on compressive strength of mortar cube specimens using finite element analysis. The analysis was conduct in an effort to explain the witnessed phenomenon of a drop in strength or decrease in the rate of strength gain observed in data collected during compression testing of actual mortar specimens. Actual compression test data from HHL2 specimens (Figure 6) illustrates this phenomenon. Prior to the 118-day compression test, there appears to be a plateau in the data (NOTE: compression testing for the HHL2 samples is incomplete since the first test occurred at 56 days, however, simple judgment would assume that the data curved in a more expected and predictable manner from 0 psi to 200 psi). The finite element results shown in Figure 5 reflect the same characteristics as the actual compression data with a strength 'plateau'

apparent in the data. It is important to note that the scales of the two plots are drastically different since there was no data available to correlate carbonation shell thickness to age of specimen. In other words, the time that the specimen takes to cure from 'no shell' to 'all shell' may occur during a short or long period of time. If the curing process does correlate to the plateau period witnessed in the actual data, then this may explain the phenomenon. For this reason, the primary future recommendation of this investigation includes an attempt to relate carbonated shell thickness to age. With this data a simple comparison could be performed to determine if the observed plateau period occurs during shell propagation or if the phenomenon is a result of some other unidentified factor.

One possible method of determining the carbonated shell thickness is by applying phenolphthalein or beet juice to a sectioned mortar specimen and observing color variations.

Another recommendation for future studies is to investigate this effect for different ratios of carbonated to un-carbonated lime. These models assumed the strength of carbonated lime to be 10 times the strength of un-carbonated lime. The compressive stiffness of carbonated lime was assumed to be 3 times that of the un-carbonated limes. It is possible, that with different strength and/or stiffness ratios, the shape of the strength gain curve will change.

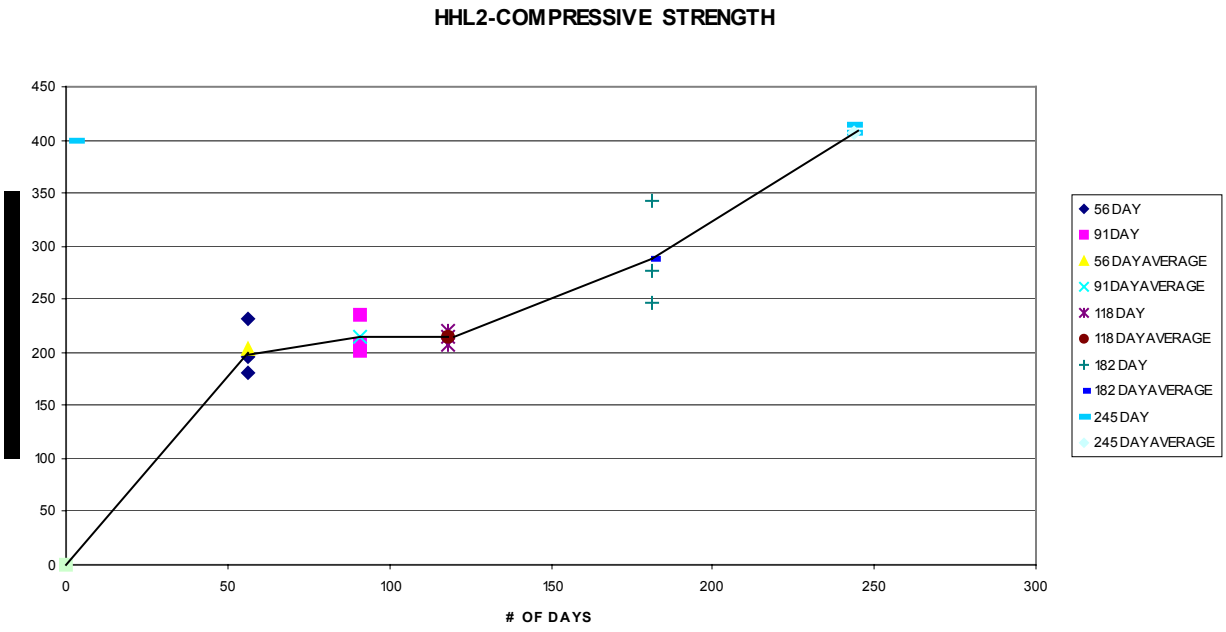

Figure 6: Actual HHL2 Compressive Strength data over time. Note that little strength gain is shown from an age of 50 to 120 days, similar to the plot of Figure 5.